UNIVERSITY OF ICELAND

B.S. Thesis
in Biochemistry and Molecular Biology

Assessing the Role of GRAMD1B in Endothelial Cell Response after Catecholamine Stimulation

Agatha Elín Steinþórsdóttir

June 2024

FACULTY OF LIFE AND ENVIRONMENTAL SCIENCES

Assessing the Role of GRAMD1B in Endothelial Cell Response after Catecholamine Stimulation

Agatha Elín Steinþórsdóttir

15 ECTS thesis submitted in partial fulfillment of a
Baccalaureus Scientiarum degree in Biochemistry and Molecular Biology

Advisors
Dr. Óttar Rolfsson
Arnar Ingi Vilhjálmsson

Faculty of Life and Environmental Sciences
School of Engineering and Natural Sciences
University of Iceland
Reykjavik, June 2024

Assessing the Role of GRAMD1B in Endothelial Cell Response after Catecholamine Stimulation
15 ECTS thesis submitted in partial fulfillment of a *B.S* degree in Biochemistry and Molecular Biology

Copyright © 2024 Agatha Elín Steinþórsdóttir
All rights reserved

Faculty of Life and Environmental Sciences
School of Engineering and Natural Sciences
University of Iceland
Sturlugata 7
102 Reykjavík
Iceland

Telephone: 525 4000

Bibliographic information:
Agatha Elín Steinþórsdóttir, 2024, Assessing the Role of GRAMD1B in Endothelial Cell Response after Catecholamine Stimulation, B.S. thesis, Faculty of Life and Environmental Sciences, University of Iceland, 55 pp.

Abstract

This research project aimed to analyse the role of the gene factor GRAMD1B in the endothelial cell response to catecholamine stimulation with a focus on its correlation to endothelial dysfunction and shock induced endotheliopathy (SHINE). Two EA.hy926 cell lines were utilized in the project, a wild-type line and a cell line with GRAMD1B knockout along with HLMVEC primary cells. Western blot analysis was used to observe changes in the expression of specific proteins of relevance to endothelial function following catecholamine stimulation. These included CA2, Thrombomodulin, ICAM-1, ICAM-2, VCAM-1, phosphorylated CREB and VEGF-A. Protein expression was observed 4-hours and 24-hours after stimulation. The results suggest a significant increase in protein expression of CA2 and Thrombomodulin in HLMVEC cells. Those findings not only help us gain a better understanding on endothelial cell function in stress but also provide a foundation for further understanding of the mechanisms behind endothelial dysfunction and SHINE.

Útdráttur

Markmið rannsóknarinnar var að skoða tengsl katekólamína við virkni æðaþelsfrumna. Rannsóknarspurning verkefnisins fólst í að svara hvort erfðaþátturinn GRAMD1B stuðli að skertri æðaþelsvirkni samhliða katekólamín áreiti, meðal annars í tengingu við sjúkdómseinkenni SHINE. Notast var við tvennskonar EA.hy926 frumulínur í verkefninu, villigerðarfrumulínu og frumulínu með GRAMD1B útslætti. Einnig voru HLMVEC frumur notaðar í verkefninu. Notast var við Western blot til að ákvarða breytingar í tjáningu á próteinunum CA2, Thrombomodulin, ICAM-1, ICAM-2, VCAM-1, fosfóleruðu CREB og VEGF-A. Flest þessara próteina eru mælikvarðar á skerta æðaþelsstarfsemi. Tjáning á próteinunum var skoðuð 4 og 24 tímum eftir katekólamín áreiti. Niðurstöður verkefnisins sýndu fram á aukna tjáningu í CA2 og Thrombomodulin í HLMVEC frumum eftir katekólamín áreiti. Þessi rannsókn gefur okkar góðan skilning á æðaþelsfrumuvirkni við aukið katekólamínáreiti og leggur grunn að betri skilningi til áframhaldandi rannsókna í tengslum við skerta æðaþelsstarfsemi og SHINE.

Table of Contents

List of Figures ..... **vii**

List of Tables ..... **ix**

Acknowledgements ..... **xi**

1 Introduction **1**
- 1.1 Vascular structure and the role of endothelium vascular homeostasis 1
- 1.2 The barrier functions of vascular endothelium 2
- 1.3 Endothelial Dysfunction is a phenotypic trait associated with vascular disease 3
- 1.4 SHINE 4
- 1.5 Previous Laboratory Findings 4
  - 1.5.1 GRAMD1B 5
  - 1.5.2 VCAM-1 5
  - 1.5.3 ICAM-1 6
  - 1.5.4 ICAM-2 6
  - 1.5.5 cAMP and CREB 6
  - 1.5.6 VEGF-A 7
  - 1.5.7 Syndecan-1 8
  - 1.5.8 Thrombomodulin 8
  - 1.5.9 CA2 9
- 1.6 Catecholamines 9
- 1.7 Aims of the Project 9

2 Materials and Methods **10**
- 2.1 Cell Culture 10
- 2.2 Catecholamine stimulation of endothelial cells and protein extraction 11
- 2.3 Bicinchoninic acid assay 12
- 2.4 Western Blot 13

3 Results **16**
- 3.1 Western blots 16
  - 3.1.1 CA2 expression was increased following adrenal stimulation 16
  - 3.1.2 Thrombomodulin expression was increased following adrenal stimulation 19
  - 3.1.3 No change in ICAM-1 expression following adrenal stimulation 22
  - 3.1.4 ICAM-2 expression was inconclusive 25
  - 3.1.5 VCAM-1 expression was inconclusive 27
  - 3.1.6 CREBp expression was inconclusive 28
  - 3.1.7 VEGF-A expression was inconclusive 31

4 Discussions **33**

References 35

List of Figures

Figure 1: Structure of a blood vessel. 1
Figure 2: Showing the function of GRAMD1B in cholesterol transportation from the cell membrane to endoplasmic reticulum. 5
Figure 3: Mechanism of the cAMP and CREB pathway. 7
Figure 4: Schematic of SHINE in acute critical ill patients. 8
Figure 5: Experimental setup for catecholamine treatment of cells. 11
Figure 6: Schematic showing the steps in BCA assay. Created with Biorender.com 13
Figure 7: Showing sandwich setup for transfer of proteins onto membranes. 15
Figure 8: Increased CA2 expression after catecholamine stimulation in HLMVEC primary cells at 4-hour timepoint. 16
Figure 9: Normalized bar graph of increased CA2 expression at 4-hour timepoint in catecholamine stimulated HLMVEC cells. 17
Figure 10: Increased CA2 expression after catecholamine stimulation in HLMVEC primary cells at 24-hour timepoint. 17
Figure 11: Normalized bar graph of increased CA2 expression at 24-hour timepoint in catecholamine stimulated HLMVEC cells. The graph indicates that there was an increase in expression after catecholamine stimulation. 18
Figure 12: Normalized bar graph with error bars showing an upregulation in CA2 expression in treated samples after 4- and 24-hour catecholamine stimulation. 19
Figure 13: Increased TM expression after catecholamine stimulation in HLMVEC primary cells at 4-hour timepoint.. 20
Figure 14: Normalized bar graph of increased TM expression at 4-hour timepoint in catecholamine stimulated HLMVEC cells.. 20
Figure 15: Increased TM expression after catecholamine stimulation in HLMVEC primary cells at 24-hour timepoint. 21
Figure 16: Non-normalized bar graph of increased TM expression at 24-hour timepoint in catecholamine stimulated HLMVEC cells. 21
Figure 17: Normalized bar graph of increased TM expression at 24-hour timepoint in catecholamine stimulated HLMVEC cells. 22
Figure 18: No change in ICAM-1 expression in EA.hy926 wild-type and knockout cell lines after catecholamine stimulation at 4-hour timepoint. 23
Figure 19 : No change in ICAM-1 expression in EA.hy926 wild-type and knockout cell lines after catecholamine stimulation at 24-hour timepoint 23
Figure 20: No change in ICAM-1 expression in EA.hy926 wild-type and knockout cell lines after catecholamine stimulation at 4-hour timepoint.. 24
Figure 21 No change in ICAM-1 expression in EA.hy926 wild-type and knockout cell lines after catecholamine stimulation at 24-hour timepoint. 24
Figure 22: Normalized bar graph of ICAM-1 protein expression at both timepoints. 25
Figure 23: ICAM-2 expression in EA.hy926 wild-type and knockout cell lines was inconclusive at 4-hour timepoint.. 25
Figure 24: ICAM-2 expression in EA.hy926 wild-type and knockout cell lines was inconclusive at 24-hour timepoint. 26
Figure 25 ICAM-2 expression in EA.hy926 wild-type and knockout cell lines was inconclusive at 4-hour timepoint. 26
Figure 26 ICAM-2 expression in EA.hy926 wild-type and knockout cell lines was inconclusive at 24-hour timepoint SMC1A 27

Figure 27: VCAM-2 expression in EA.hy926 wild-type and knockout cell lines was inconclusive at 4-hour timepoint. 28
Figure 28: VCAM-2 expression in EA.hy926 wild-type and knockout cell lines was inconclusive at 24-hour timepoint. 28
Figure 29: CREBp protein expression in EA.hy926 wild-type and knockout cell lines was inconclusive at 4-hour timepoint. 29
Figure 30: CREBp protein expression in EA.hy926 wild-type and knockout cell lines was inconclusive at 24-hour timepoint. 29
Figure 31: CREBp protein expression in EA.hy926 wild-type and knockout cell lines was inconclusive at 4-hour timepoint. 30
Figure 32 CREBp protein expression in EA.hy926 wild-type and knockout cell lines was inconclusive at 24-hour timepoint. 30
Figure 33:VEGF-A protein expression in EA.hy926 wild-type and knockout cell lines was inconclusive at 4-hour timepoint. 31
Figure 34: VEGF-A protein expression in EA.hy926 wild-type and knockout cell lines was inconclusive at 24-hour timepoint. 32

List of Tables

Table 1: Showing quantification of adrenaline and nor-adrenaline in catecholamine mix. 12
Table 2: Dilution of BSA for determination of standard curve. Scheme found via (*Pierce^{TM} BCA Protein Assay Kits*, n.d.). 13
Table 3: Western blot sample preparation. 14
Table 4: Antibodies used in project. 15

Acknowledgements

First and foremost, I would like to express my deep gratitude to my advisor, Dr. Óttar Rolfsson, for giving me the opportunity to join his research project and for his invaluable advice and guidance throughout. I would also like to express my gratitude to Arnar Ingi Vilhjálmsson, who has helped me immensely in the project, by teaching me valuable research skills inside and outside the lab. I am thankful for the experience of working alongside brilliant scientists in the lab. Finally, I would like to thank my fellow Biochemistry and Molecular Biology friends for their support over the last three years.

1 Introduction

1.1 Vascular structure and the role of endothelium vascular homeostasis

Blood vessels comprise of three layers, tunica externa, tunica media and tunica intima (*figure 1*). Tunica externa is the outermost layer of the blood vessel, consisting of collagen-rich extra cellular matrix, and fibroblasts. The external membrane consists of elastin for flexibility (Witter et al., 2017). The middle layer of the blood vessel is called the tunica media, which consists of smooth muscle cells in a collagen fiber network. The innermost layer, called the tunica intima comprises endothelial cells, basal lamina and the internal membrane, which consist of elastin (Mozafari et al., 2019).

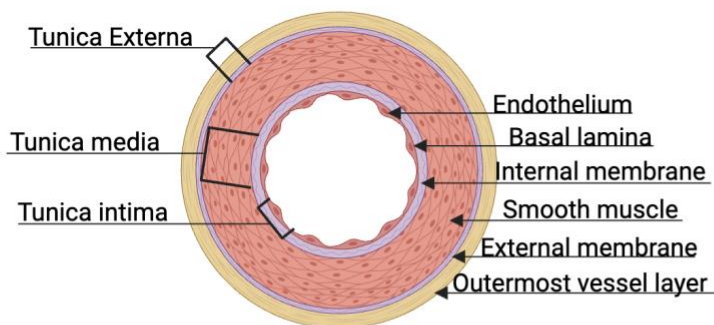

Figure 1: Structure of a blood vessel. Created with Biorender.com.

The endothelium plays a crucial role in homeostasis, with both smooth muscle cells and endothelial cells expressing proteins that take part in the process (Konukoglu & Uzun, 2017).The endothelium is considered as a whole organ system that takes part in numerous physiological functions (Aird, 2004). Endothelial cells line the entire vascular system, which is called the endothelium and is crucial for vascular function and blood supply (Alberts et al., 2002). The vascular endothelium is the main regulator for vascular homeostasis and takes part in interacting with circulating blood cells and molecules, which

makes it exposed to changes in the blood composition and flow. Healthy endothelium consists both of anticoagulant and antithrombotic factors, which the endothelial cells secrete. Shifts in concentration of these factors, for example due to inflammation, may lead to a change in regulation of blood coagulation and platelet function. (Michiels, 2003).

1.2 The barrier functions of vascular endothelium

The endothelium possesses a barrier which works as a regulator for the transport of macromolecules and blood elements which can differ in permeability, due to intercellular junctions (Dyer & Patterson, 2010). There are three described cell-to-cell junctions in the endothelium, tight, adherens and gap junctions. Tight junctions regulate the diffusion of molecules into regions between cells. Also, they have ability to control cellular polarity by restricting the distribution of lipids in the membrane. Adherens junctions are found right underneath the tight junctions on the cell. They consist of nectin-based adhesions, which have the ability to make a connection between neighbouring cells, and lastly cadherins junctions, they form strong cell-to-cell adhesion by the binding to catenin (Campbell et al., 2017). Gap junctions are channels that lie outside the cell and connect to the cytoplasm of neighbouring cells, that allows direct intracellular contact between cells. Endothelial cells and smooth muscle cells use gap junctions as a mediator for electrical communication that is important for vasomotor toning (Figueroa & Duling, 2009).

The endothelial glycocalyx lines the vascular endothelium and is composed of proteoglycans and glycoproteins which connect the glycocalyx to the endothelium (Reitsma et al., 2007). The endothelial glycocalyx has important roles in vascular permeability, regulating leukocyte and platelet interactions with adhesion cell molecules on the surface of the endothelium. The glycocalyx is in contact with flowing blood which makes it susceptible to changes in blood composition, which can be trauma induced. Changes in vascular permeability, caused by pathological conditions can lead to shedding of the glycocalyx. Trauma patients have shown to have biomarkers which point to glycocalyx shedding. Syndecans are proteoglycans and are part of the glycocalyx composition. The syndecan family is composed of four groups and a few isomers. Syndecan-1 is a biomarker for degradation of the glycocalyx, frequently noticed in blood composition. High circulating syndecan-1 has shown to be associated with coagulopathy,

mortality in acute ill patients and shock induced endotheliopathy (SHINE) (Chignalia et al., 2016). Thrombomodulin is a glycoprotein which is located on the endothelial glycocalyx. It takes part in regulating homeostasis in the cell. Dissociation of thrombomodulin from the glycocalyx can lead to a disruption in coagulation. Thrombomodulin is a biomarker, often found as a circulating marker in the blood in acute ill patients and SHINE (further expanded in sections 1.4) (Britten et al., 2021).

1.3 Endothelial Dysfunction is a phenotypic trait associated with vascular disease

Endothelial dysfunction is described as a change in the mechanism of the endothelium and accompanies reduced vasodilation, increased inflammation, and prothrombic activity (Endemann & Schiffrin, 2004). It is not only a deterioration of the vasodilation in the endothelium, but also abnormalities in the interactions between the endothelium and leukocytes, thrombocytes, and regulatory molecules (Konukoglu & Uzun, 2017). Recent studies have shown that endothelial dysfunction is associated with numerous conditions, including cardiovascular diseases such as heart failure, diabetes and hypertension (Endemann & Schiffrin, 2004).

Endothelial dysfunction is also affiliated with increased vascular permeability, oxidative stress which leads to loss of vascular toning (López García de Lomana et al., 2022). Healthy endothelial cells express molecules which have a protective role by prohibiting platelet clustering and the formation of fibrin. Those molecules have antiplatelet and anticoagulant abilities. Healthy endothelium inhibits the adhesion of leukocytes and migration. If an injury occurs to the endothelium, those molecules lose their protecting abilities, that can lead to the appearance of adhesive and pro-coagulant function in the endothelium. Endothelial dysfunction exhibits a decrease in nitric oxide availability, injury to the smooth muscle cells regarding vasodilation and increased sensitivity to vasoconstrictable molecules and shear stress. Oxidative stress has a strong correlation with the metabolism of nitric oxide, which has a destructive effect on the endothelium (Konukoglu & Uzun, 2017).

Endothelial dysfunction is liable for inflammation and blood coagulation which can lead to thrombosis. TNF-alpha and IL-1 have a decreasing effect on the expression of thrombomodulin, nitric oxide and prostacyclin. (Konukoglu & Uzun, 2017).

1.4 SHINE

Shock induced endotheliopathy (SHINE) is a proposed pathophysiological disease which occurs in acute critical ill patients. Approximately one quarter of patients suffering from acute critical illness develop coagulopathy, which is a condition associated with a significant increase in mortality. Sympatho-adrenal hyperactivation, which is the body's response to shock in acute critical ill patients, leads to damage to the endothelial cells and shedding of the glycocalyx. The glycocalyx lines the blood vessels and inhibits coagulation and regulates vessel permeability. This hyperactivation leads to an increase in catecholamine levels, which leads to damage of to the endothelium, as well as the shedding of glycocalyx, breakdown of tight-junctions and leakage of capillaries. This state drives a reduction on oxygen delivery which can lead to multiple-organ failure and death (P. Johansson et al., 2017).

1.5 Previous Laboratory Findings

Previous research had been conducted by the Rolfsson Lab in the last years which was used as a foundation in the student's project. Endothelial dysfunction and SHINE have been linked to high adrenaline plasma concentrations in acute ill patients that have suffered from some type of shock. The lab has been conducting research based on adrenaline stimulation of endothelial cells to simulate biological responses in acute ill patients during shock. RNA sequencing was conducted on endothelial cells stimulated with catecholamines, the data from that experiment revealed that GRAMD1B was highly upregulated. To elucidate the role of GRAMD1B in endothelial dysfunction and SHINE, a GRAMD1B knockout cell line was established in the immortalized endothelial cell line EA.hy926. One outstanding question is whether or not GRAMD1B influences the expression of known biomarkers of endothelial dysfunction and SHINE. In the next following sections I describe these biomarkers as assessing their differential expression was a main of this work, further expanded in the following sections.

1.5.1 GRAMD1B

Cholesterol is an abundant membrane lipid which plays a pivotal role in cell signalling and the firmness of cellular membranes. The cell membrane is abundant of cholesterols that are synthesized in the endoplasmic reticulum (ER). Cells can detect an elevation in cholesterol in the cell membrane, which activates the transportation of it to the ER. GRAMD1B is a cholesterol transport molecule which transports cholesterol from the cell membrane to the endoplasmic reticulum, see *figure 2* (Naito & Saheki, 2021). In case of low cholesterol levels, Insig proteins act as a negative regulator for cholesterol synthesis by activating SREBp cleavage-activating protein (SCAP) and sterol regulatory element binding proteins (SREBp) which prohibit the passage of the SCAP-SREB complex to the Golgi apparatus, therefore inhibiting the transcription of cholesterol target genes, which take part in synthesis of fatty acids and cholesterols (McFarlane et al., 2014).

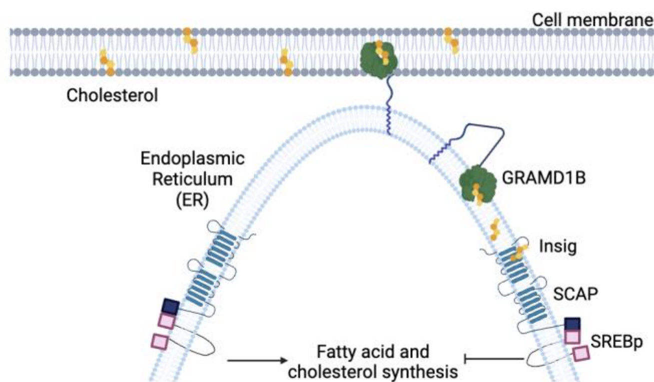

Figure 2: Showing the function of GRAMD1B in cholesterol transportation from the cell membrane to endoplasmic reticulum. On the left, figure shows how cholesterol synthesis is regulated, and on the right, how synthesis in inhibited by Insig, SCAP and SREBp Created with Biorender.com.

1.5.2 VCAM-1

Adhesion molecules are important for cellular function and homeostasis. The adhesion receptors take part in cell-to-cell interactions which trigger signalling cascades in the cell (Bui et al., 2020). Vascular cell adhesion molecule-1 (VCAM-1) is a surface glycoprotein which is mostly expressed in endothelial cells, though it can be expressed in other cell types like tissue macrophages under high levels of inflammation. The expression is activated by pro-inflammatory cytokines like TNFα and reactive oxygen species (ROS). VCAM-1 expresses Ig-like domains. Ig-like domains 1 and 4 take part in ligand binding, for instance α4ß1 integrin, and is important for leukocyte adhesion to the endothelium.

α4ß1 integrin binds to VCAM-1 on the endothelial cells which allows migration of leukocytes through the endothelium (Kong et al., 2018).

1.5.3 ICAM-1

Intercellular adhesion molecule-1 (ICAM-1) is a surface glycoprotein which acts as a recruiter for leukocytes during inflammation. ICAM-1 is expressed in low amount in endothelial cells but is upregulated during inflammation as a response to inflammatory cytokines. ICAM-1 functions as a regulator for leukocyte transendothelial migration (TEM) which makes possible for leukocytes to cross the endothelial barrier, which has been studied in relation to epithelial injury response during inflammation (Bui et al., 2020). ICAM-1 has been studied in relations to acute critical illness as marker for endothelial dysfunction, where it acts as a circulating adhesion molecule (López García de Lomana et al., 2022).

1.5.4 ICAM-2

Intercellular adhesion molecule-2 (ICAM-2) is a transmembrane glycoprotein and is expressed in the endothelium. It is a protein which takes part in vascular permeability, it regulates the flux of liquid inside the vessels and tissue. This process is important for tissue health and adaption to changes in blood pressure and inflammation. The expression is frequently due to cytokine stimulation (Martz, 1998). This protein is important for antigen-specific immune response, as it mediates adhesive interactions. Additionally, it is essential in lymphocyte recirculation as blocks of LFA-1 cell adhesion (*ICAM2 - Intercellular Adhesion Molecule 2 - Homo Sapiens (Human) | UniProtKB | UniProt*, n.d.). ICAM-2 controls the localization of N-cadherin, which is an adhesion molecule located at the endothelial junctions (Amsellem et al., 2014).

1.5.5 cAMP and CREB

Cyclic adenosine monophosphate (cAMP) functions as a second messenger in signalling pathways. It is synthesized from ATP by adenylyl cyclase enzyme. Increased cAMP concentration in the cell leads to the activation of G protein coupled receptors (GPCR) which are coupled to stimulatory G protein therefore activating adenylyl cyclase (Alberts et al., 2022). Catecholamines are signal molecule which bind to GPCR, activating the cAMP cascade (Andreis & Singer, 2016). Adenylyl cyclase activates the conversion of ATP to cAMP, which leads cAMP to activate protein kinase A (PKA). PKA consists of 4

subunits, two catalytic and two regulatory. PKA phosphorylates serines and threonines on specific target proteins, such as intracellular signalling proteins. Activated PKA phosphorylates CRE-binding protein (CREB) in the nucleus, which recognizes the cyclic AMP response element (CRE) (Zhang et al., 2020). CRE-binding protein (CREB) recognizes the CRE sequence which initiates the transcription of specific target genes like VEGF (Alberts et al., 2022).

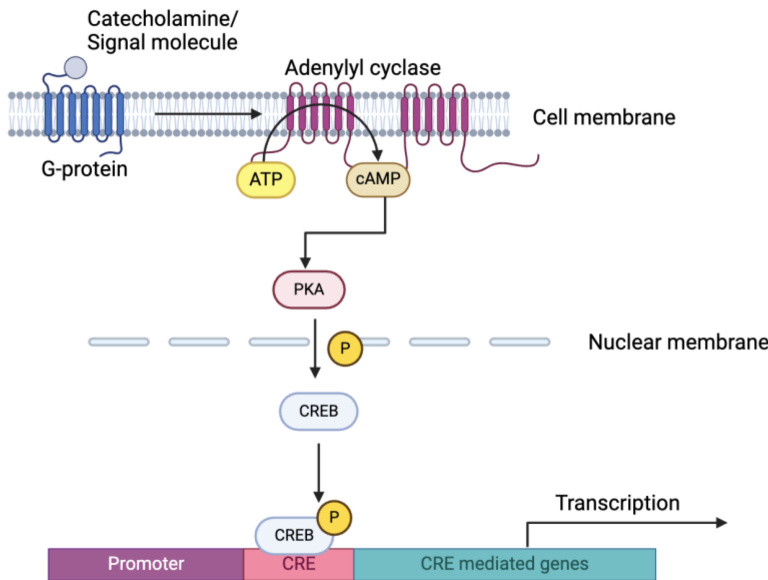

Figure 3: Mechanism of the cAMP and CREB pathway. Showing how signal molecules, for example catecholamines can stimulate the activation of G-proteins, which leads to activation of adenylyl cyclase. Therefore activating phosphorylation cascade which ends by the binding of phosphorylated CREB to CRE binding sites and initiate the transcription of CRE mediated genes. Created with Biorender.com.

1.5.6 VEGF-A

Vascular endothelial growth factor (VEGF) is a key regulator and essential growth factor in endothelial cells. VEGF-A is a polypeptide which binds to the tyrosine kinase VEGF receptor on the cell membrane (Eichmann & Simons, 2012). Vascular endothelial growth factor induces angiogenesis but can also have a deteriorating effect on the vascular barrier in ischaemic tissue. VEGF takes part in uncoupling endothelial cell-to-cell junctions which leads to increased vascular permeability (Weis & Cheresh, 2005). VEGF-A is endothelial growth factor in the VEGF family and induces the formation of new blood vessels. This growth factor takes particularly part in vascular permeability (Nagy et al., 2007).

1.5.7 Syndecan-1

Syndecan-1 is a transmembrane heparin-sulfate proteoglycan which is expressed in endothelial cells. Syndecan-1 is located within the glycocalyx, which is a layer on top of endothelial cells. The glycocalyx is a negative charged layer of proteoglycans and glycoproteins, for example ICAM-1, ICAM-2, and VCAM-1. The glycocalyx plays a pivotal role in vascular permeability. In case of deterioration, it can result in capillary leaks, exposing endothelial cells to circulating platelets and leukocytes, which trigger inflammatory response and disrupts coagulation processes (Gonzalez Rodriguez et al., 2017). Circulating syndecan-1 is a marker for deterioration of the glycocalyx and endothelial dysfunction (P. I. Johansson et al., 2011). Syndecan-1 is a biomarker for SHINE in trauma patients. A correspondence between circulating syndecan-1 and high plasma adrenaline has been showed in relation to breakdown of the endothelium, which leads to capillary leakage and reduced oxygen delivery (P. Johansson et al., 2017).

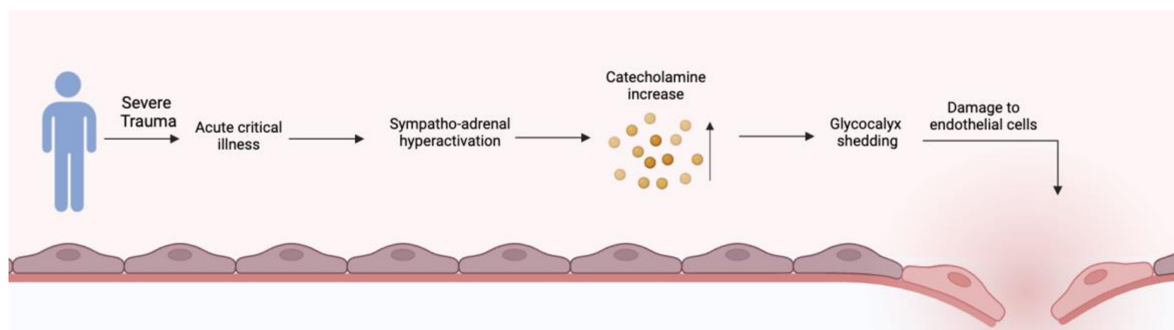

Figure 4: Schematic of SHINE in acute critical ill patients. Showing how acute critical illness in trauma patients has an increasing effect on catecholamines which leads to damage to the endothelial cells. Created with Biorender.com.

1.5.8 Thrombomodulin

Thrombomodulin (TM) is a transmembrane proteoglycan, which functions as a thrombin receptor at the surface on endothelial cells (Boffa & Karmochkine, 1998). Thrombin is a procoagulant enzyme, which thrombomodulin can enzymatically cleave converting it to an anticoagulant molecule via the protein C pathway (Reitsma et al., 2007). Thrombomodulin plays an important role as a natural anticoagulant. During cytokine stimulation, thrombomodulin is cleaved and soluble parts are released into the blood stream (Boffa & Karmochkine, 1998). High levels of catecholamines contribute to high levels of circulating thrombomodulin in the blood stream and is a described biomarker for SHINE (P. Johansson et al., 2017).

1.5.9 CA2

Carbonic anhydrases (CA) are enzymes which have origin in the mitochondria and take part in the reversible conversion of bicarbonate ions and water into carbon dioxide. CA are involved in diverse biological processes like pH homeostasis, CO_2 transport, gluconeogenesis and lipogenesis. CA regulate oxidative metabolism of glucose in the cell and control the rate of production of reactive oxygen species (Shah et al., 2013).
The endothelium is a metabolic active organ which relies mainly on glycolysis for ATP production (De Bock et al., 2013). Fifteen CA enzymes have been described in mammals (Alver et al., 2011). Recent studies have shown that carbonic anhydrase 2 is upregulated in catecholamine stimulated endothelial cells.

1.6 Catecholamines

Adrenaline, noradrenaline, and dopamine are molecules known as catecholamines and are vital for sustaining homeostasis in the cell. All catecholamines are derived from the hydroxylation of tyrosine which yields dopamine and noradrenaline, further modification of noradrenalin by methyltransferase yields adrenaline (Paravati et al., 2024).
Catecholamines are released into the bloodstream following the activation of adrenergic synapses between neurons in the body (Andreis & Singer, 2016).
In response to stress in shocked or injured patients, adrenaline and noradrenaline are released. Activation of the sympatho-adrenal system triggers the release of catecholamines into the bloodstream, potentially leading to coagulopathy in patients (P. Johansson et al., 2017).

1.7 Aims of the Project

The aim of the project was to assess if GRAMD1B influences the expression on VCAM-1, ICAM-1, ICAM-2, thrombomodulin, CA2 and phosphorylated CREB proteins in endothelial cells following catecholamine stimulation. The focus was on antibody screening by Western blots. The primary research question addressed in the project was whether GRAMD1B upregulates the expression of those proteins following catecholamine stimulation.

2 Materials and Methods

2.1 Cell Culture

Two cell lines, wild-type and GRAMD1B knockout EA.hy926 lines as well as HLMVEC primary cells were used in the experiments. EA.hy926 is a immortalized cell line, formed by the fusion between Human Umbilical Vein Endothelial Cells and a thioguanine-resistant clone of A549 (*EA.Hy926 - CRL-2922 | ATCC*, n.d.). The primary cells, Human Lung Microvascular Endothelial Cells (HLMVEC) were purchased from Lonza (CC-2527) and were cultured in EGM-2 MV Microvascular Endothelial Cell Growth Medium-2 BulletKit (CC-3202). The cell line EA.hy926 was purchased from ATCC (CRL-2922) and cultured in Dulbecco's Modified Eagle Medium (DMEM/F-12) (Gibco, 11320033) with 10% Fetal Bovine Serum (FBS) (Gibco, A5256701) and 40 U/mL of Penicillin-Streptomycin (P/S) (Gibco, 15140122). The Ea.hy926 GRAMD1B knockout cell line had already been established at our lab and was cultured in the same growth media as the wild-type cell line.

Cells were grown in T25 or T75 cell culture flasks (Falcon) and incubated at 37°C, 5% CO_2. Cells were passaged at 80-90% confluency, the growth media was aspirated, and the cells were rinsed with 1x PBS (Gibco, 18912014). The 1x PBS was then aspirated and 1x Trypsin (Gibco, 15400054) was added to the cells and incubated for 10 minutes in the incubator. When the cells were loose, they were resuspended in warm growth media. The cell suspension was then split into new cell culture flasks. Split ratios were; HLMVEC 1:2, EA.hy926 Wild-type 1:4 every other day and 1:8 over weekends, EA.hy926 GRAMD1B knockout 1:3 every other day and 1:6 over weekends. Before use, 1x Trypsin and DMEM was warmed up to 37°C. 1x PBS was used at room temperature. Cell culture was carried out in sterile environment in a laminar flow-hood.

2.2 Catecholamine stimulation of endothelial cells and protein extraction

Cells were cultured in T25 flask and then later expanded into a T75 flask. When cells were confluent enough, they were ready for seeding. Cells were disassociated as described in Chapter 2.1 and the cell suspension was moved to a 15 mL Falcon tube. Cell suspensions were centrifuged at 180 RCF for 5 minutes. The media was aspirated from the cell pellet before being resuspended in 5 mL of growth media. 10 µL of the cell suspension was placed into two slots on an Improved Neubauer Hemocytometer and the concentration of the cell suspension calculated. 300.000 cells were seeded into each well of a 6 well plate. Varied number of plates were used in the seeding, due to different cell lines and timepoints. Usually, six plates were used when seeding both the wild-type and knockout EA.hy926 cell lines, but only two for the HLMVEC cells (*figure 5)*. The cells were then incubated at 37°C, 5% CO_2 for 72 hours. After 72 hours the media was aspirated from all wells and 2 mL of fresh growth media was added to each well, the cells were then incubated for 24 hours before being treated.

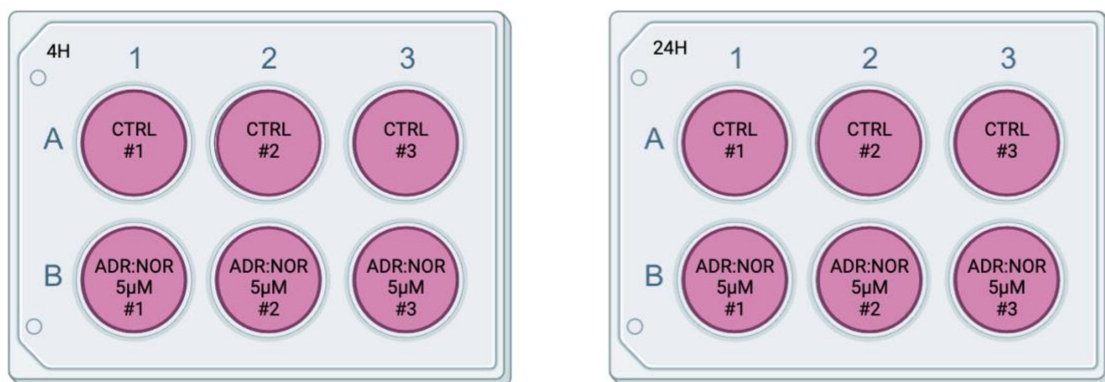

Figure 5: Experimental setup for catecholamine treatment of cells. Both plates represent each timepoint in the catecholamine treatment. Three technical triplicates were made, both for control and catecholamine stimulated samples (ADR:NOR). Created with Biorender.com.

Adrenaline and Noradrenaline were weighed and resuspended in 2 mL of 1M HCl (*table 1*). 10 µL of both the Adrenaline and Noradrenaline solutions were diluted in 10 mL of growth media to create a 50 µM equimolar solution, this was diluted to a working concentration of 5 µM. Cells were assayed at two timepoints following treatment at 4-hours and 24-hours, respectively. Each experiment consists of three technical replicates for each treatment condition. When cells were treated, the media was aspirated from each well

and 2 mL of the appropriate treatment mix was added. For the control conditions, 2 mL of growth media was added without catecholamines.

After treating the cells, the media was collected in 2 mL Eppendorf tubes and stored at -20°C. The cell monolayer was rinsed with 1x PBS and kept on ice. The 1x PBS was aspirated from the cell monolayer and 100 µL of Pierce RIPA buffer (Thermo Scientific, 89900) containing 1x Halt Protease and Phosphatase Inhibitor Cocktail (Thermo Scientific, 78446). The cells were scraped using a cell scraper and the lysate was moved to 1,5 mL Eppendorf tubes. All samples were centrifuged at 16.000 RCF for 5 minutes and the supernatant was then moved to a new Eppendorf tube and stored at -20°C.

Table 1: Showing quantification of adrenaline and nor-adrenaline in catecholamine mix.

Component	Weight (mg)	Weight (g)	Moles
Adrenaline (E4250-1G)	18,3 mg	0,0183	9,99454E-05
Noradrenaline (A7257-1G)	16,9 mg	0,0169	9,99409E-05

2.3 Bicinchoninic acid assay

Bicinchoninic acid assay (BCA) was performed to determine protein quantification in each of the cell lysate samples. Pierce™ BCA Protein Assay Kit was utilized in this assay (*Pierce™ BCA Protein Assay Kits*, n.d.). BCA assay uses bicinchoninic acid for colorimetric detection for the quantification of proteins. The structure and size of proteins initiate the purple colour formation which occurs in BCA. Firstly, BCA a standard curve is determined, which is done by series of dilution of a known protein, like Bovine Serum Albumin (BSA). Which can then be used as a standard comparable to the unknown protein concentrations (see *Table 4*). At first unknown protein samples were diluted, 9 µL of sample to 91 µL of ddH_2O. Next up, 25 µL of unknown protein and standard curve samples were loaded into a 96 well plate, technical triplicates were made for each sample for comparison. Then, 200 µL of BCA solution was added to the wells and plate incubated at 37°C for 30 minutes. The plate was read by a spectrophotometer at 562 nm absorbance, see *figure 6* for reference. The results were calculated using Excel.

Table 2: Dilution of BSA for determination of standard curve. Scheme found via (*Pierce™ BCA Protein Assay Kits*, n.d.).

Dilution Scheme for Standard Test Tube Protocol and Microplate Procedure (Working Range = 20–2,000 µg/mL)			
Vial	Volume of Diluent (µL)	Volume and Source of BSA (µL)	Final BSA Concentration (µg/mL)
A	0	300 of Stock	2000
B	125	375 of Stock	1500
C	325	325 of Stock	1000
D	175	175 of vial B dilution	750
E	325	325 of vial C dilution	500
F	325	325 of vial E dilution	250
G	325	325 of vial F dilution	125
H	400	100 of vial G dilution	25
I	400	0	0 = Blank

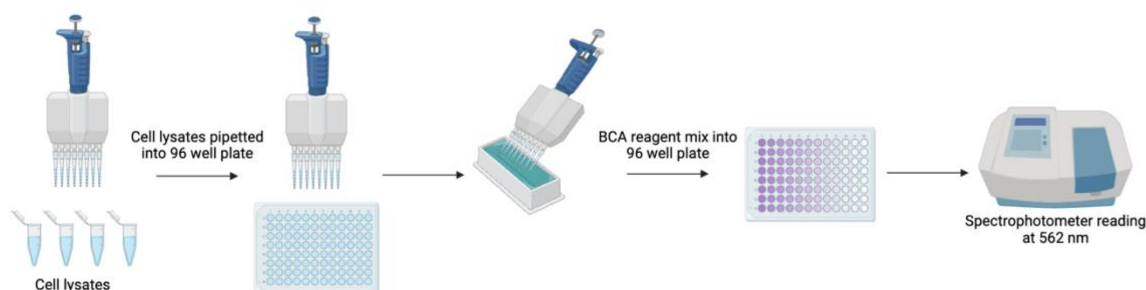

Figure 6: Schematic showing the steps in BCA assay. Created with Biorender.com

2.4 Western Blot

The samples used for western blotting were stored at -20°C and thawed at room temperature before use. Protein concentration had already been determined via BCA assay, therefore samples could be loaded with equal protein concentration onto the SDS gels. Bolt Bis-Tri Plus Mini Protein Gels, with a 4-12% gradient, 1,0 mm, WedgeWell Format (Invitrogen, NW04120BOX) were used for Western blots.

Samples were prepared according to *table 3*. Tubes were centrifuged briefly to collect samples at the bottom and then denatured at 70°C for 10 minutes. Gels were removed from their packaging, rinsed with ddH_2O and placed into the tank. 50 mL of Running buffer (#B0001, Thermo Scientific) and 950 mL of ddH_2O solution was prepared and poured into the tank. 3 µL of protein ladder (#26616, Thermo Scientific) was loaded into the first well and 1.5 µL into the last well. Then, 20 µL of each sample was loaded into rest of the wells. The gels were run at 180V for one hour. After running the gel, the proteins were transferred to a Nitrocellulose Pure Transfer membrane (#88018, Thermo Scientific). Transfer was done by assembling a transfer sandwich as shown in *figure 7*. The transfer sandwich was placed into the tank along with a solution of 50 mL of Transfer buffer (#BT00061, Thermo Scientific), 200 mL of methanol and 750 mL of ddH_2O. The transfer

was run at 28V for 90 minutes. After the transfer, the membranes were removed and washed with ddH_2O and blocked in 5 % milk for 1-2 hours. Primary antibodies, shown in *table 4*, were mixed in blocking buffer and incubated at 4 °C overnight on a shaker. Primary antibodies were removed and put back into their falcon tubes and stored at -20 °C for reuse. The membranes were washed with 1xTBST for 10-15 minutes, which was repeated 3-4 times. Meanwhile, secondary antibodies were mixed in blocking buffer. After washing, the secondary antibody was put onto the membrane and incubated for one hour at room temperature on a shaker. After incubating, the membrane was washed again for 10-15 minutes, 3-4 times. Meanwhile, Western Blot Luminol Reagent (#34580, Thermo Scientific) was mixed into 1:1 ratio. After washing, each membrane was lightly washed in ddH_2O and placed in a box containing the Luminol Reagent and incubated for 3 minutes. After incubation, the membrane was moved onto a plastic sleeve and imaged using Bio-Rad Universal Hood 2 Gel Doc System with Image Lab software.

Table 3: Western blot sample preparation.

Components	**Reduced sample**
Sample	X µL
Bolt LDS Sample Buffer (4X)	5,5 µL
Bolt Reducing Agent (10X)	2,2 µL
ddH_2O	Up to 14,3 µL
Total Volume	**22 µL**

Figure 7: Showing sandwich setup for transfer of proteins onto membranes. Created with Biorender.com

SMC1A and Beta-tubulin were used as housekeeping genes as they do not respond to treatment used in the project.

Table 4: Antibodies used in project.

Target	Host	Type	Dilution	Company	Cat#
SMC1A	Rabbit	Primary	1:1000	Abcam	AB9262
Beta-tubulin	Rabbit	Primary	1:1000	Cell signalling	2128
CA2	Rabbit	Primary	1:1000	Abcam	ab124687
CREBp	Rabbit	Primary	1:4000-1:8000	Proteintech	28792-1-AP
ICAM-1	Rabbit	Primary	1:6000	Proteintech	10931-1-AP
ICAM-2	Rabbit	Primary	1:500-1:1000	Proteintech	10121-2-AP
VCAM-1	Rabbit	Primary	1:1000	Proteintech	66294-1-IG
Thrombomodulin	Rabbit	Primary	1:1000	Proteintech	14318-1-AP
VEGFA	Rabbit	Primary	1:1000	Abcam	AB46154
HRP-Goat Anti-Rabbit recombinant	Rabbit	Secondary	1:10000	Proteintech	RGAR001

3 Results

3.1 Western blots

Western blots were used to establish changes of proteins in control samples and samples stimulated with adrenaline and noradrenaline for 4 hours and 24 hours. HLMVEC primary cells and EA.hy926 wild-type and knockout cell lines were used in the Western blots. All protein expression intensities were normalized to the expression intensities of SMC1A.

3.1.1 CA2 expression was increased following adrenal stimulation

Protein expression of Carbonic Anhydrase 2 (CA2) was analyzed after both timepoints in HLMVEC primary cells in comparison to the control samples. A western blot was performed after both timepoint, 4-hours (*figure 8*) and 24-hours (*figure 10*). The blot for the 4-hour timepoint shows unequal loading in well 3, labeled 'Control 3' in the SMC1A. Unspecific bands were present above the SMC1A protein expression. Nearly equal loading was established in all treated samples. CA2 protein expression was only present in the treated samples.

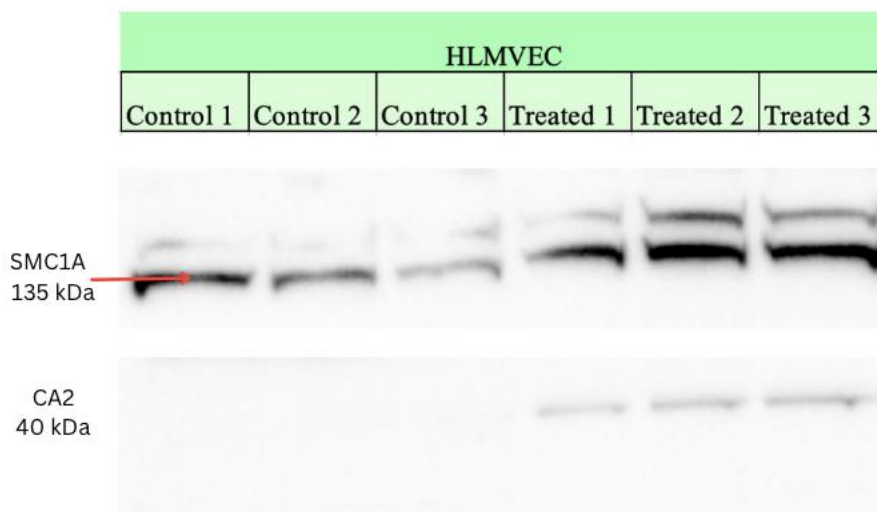

Figure 8: Increased CA2 expression after catecholamine stimulation in HLMVEC primary cells at 4-hour timepoint. Western blots showing protein expression of SMC1A housekeeping gene at 135 kDa, which was used as a standard. Carbonic Anhydrase 2 protein expression is not present in control groups but present after catecholamine stimulation. Expression of CA2 is at around 40 kDa, which is the same as the academia states.

Figure 9 shows a bar graph with normalized protein expression of CA2 at the 4-hour timepoint. The blot showed an upregulation of CA2 after catecholamine stimulation. There

was some CA2 expression in control sample 3, which could be caused by contamination between samples since there is no expression in the other control samples.

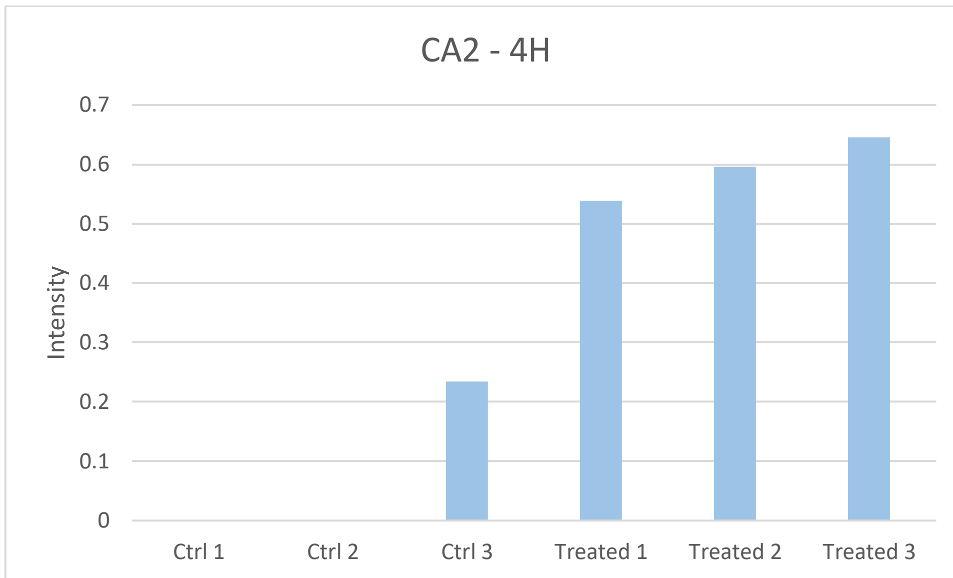

Figure 9: Normalized bar graph of increased CA2 expression at 4-hour timepoint in catecholamine stimulated HLMVEC cells. The graph indicates that there was an increase in expression after catecholamine stimulation. There was also some expression in control sample 3.

Figure 10 shows CA2 protein expression after the 24-hour catecholamine stimulation timepoint. SMC1A was used as a reference protein, which indicated adequate loading of samples in each well. CA2 expression was only detected in the catecholamine stimulated samples.

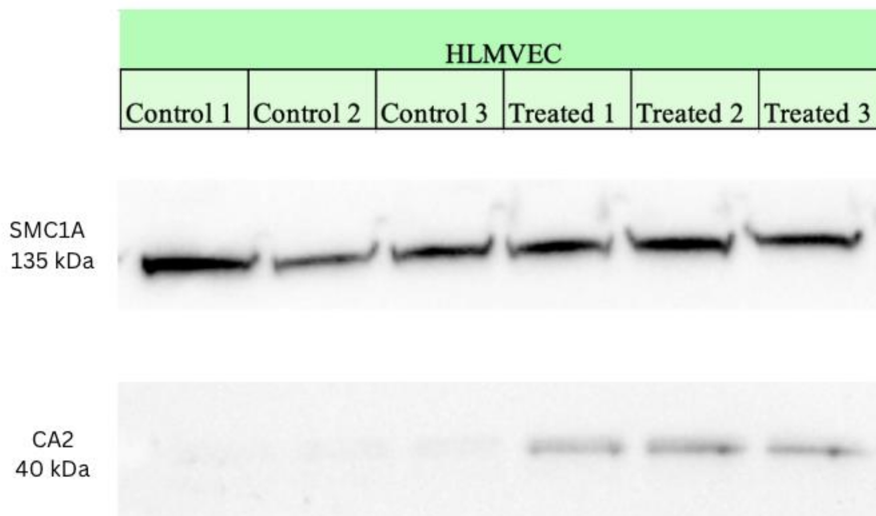

Figure 10: Increased CA2 expression after catecholamine stimulation in HLMVEC primary cells at 24-hour timepoint. SMC1A protein expression was proper with expression around 135 kDa. CA2 protein expression was detected around 40 kDa. Bands were only detected in catecholamine stimulated samples.

Figure 11 shows a bar graph with normalized protein expression of CA2 at the 24-hour timepoint. The graph shows a clear increase in expression of proteins in treated samples.

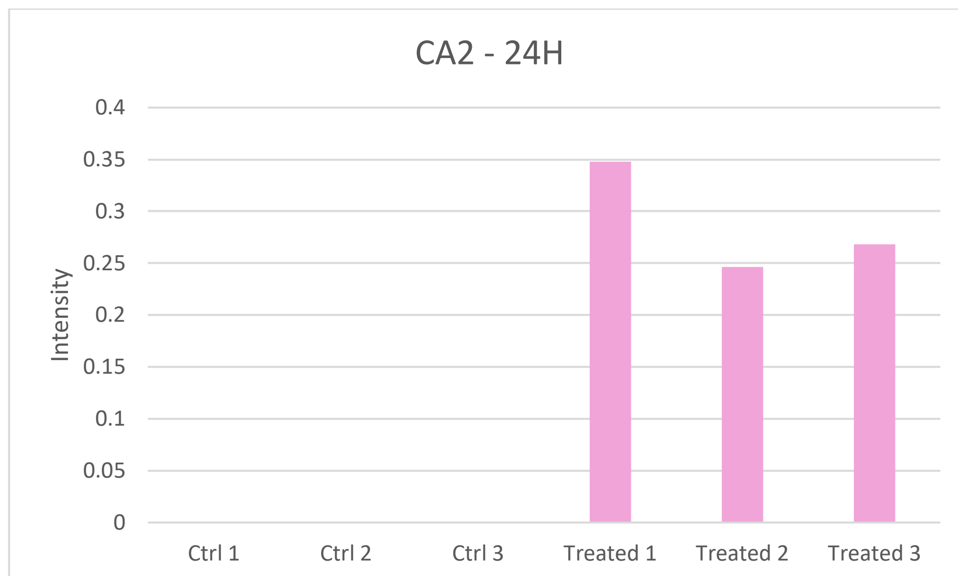

Figure 11: Normalized bar graph of increased CA2 expression at 24-hour timepoint in catecholamine stimulated HLMVEC cells. The graph indicates that there was an increase in expression after catecholamine stimulation.

Figure 12 shows a normalized bar graph of protein expression at both timepoints with error bars. The graph shows a decrease in CA2 expression between the two timepoints, which can be an indicator of uneven loading of samples between blots. It can also be interpreted as a decrease in the protein expression in the cells themselves after longer catecholamine stimulation. Error bars show a standard deviation from the data and how much the data deviates from the mean value.

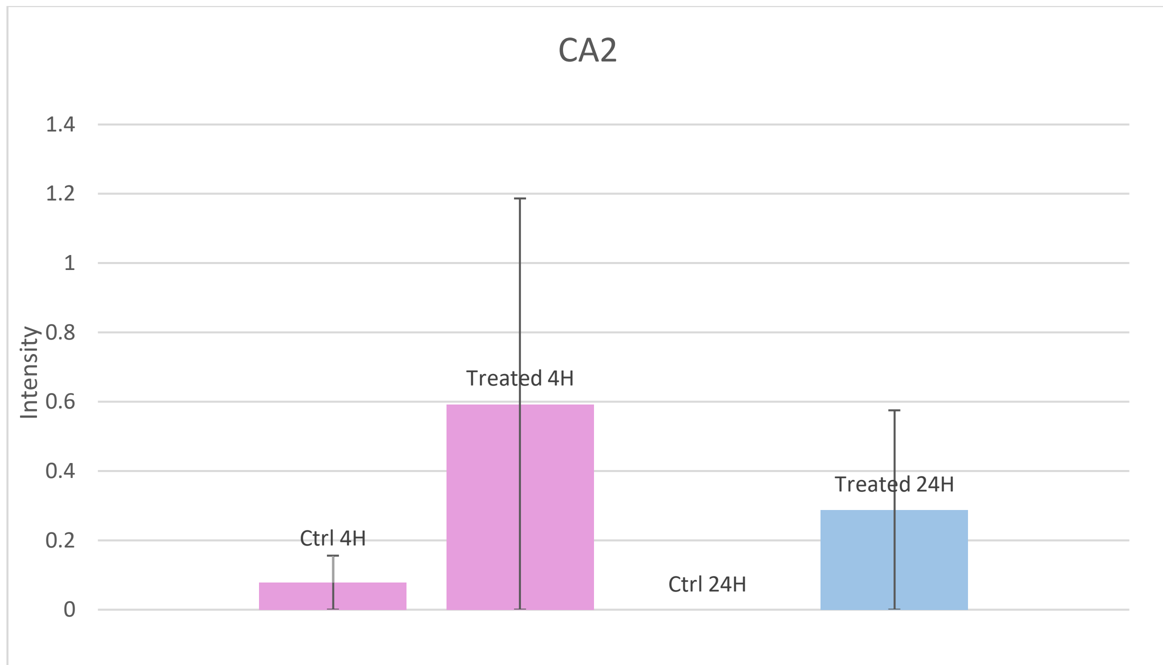

Figure 12: Normalized bar graph with error bars showing an upregulation in CA2 expression in treated samples after 4- and 24-hour catecholamine stimulation. In both timepoints is there an increase in protein expression in treated samples compered to control. This might indicate an upregulation in CA2 after stimulation.

3.1.2 Thrombomodulin expression was increased following adrenal stimulation

Protein expression of thrombomodulin (TM) in HLMVEC primary cells was analyzed at both timepoints after catecholamine stimulation. *Figure 13* shows an equal expression of SMC1A at the 4-hour timepoint at 135 kDa. TM expression was detectable in all samples with an increase in catecholamine stimulated samples. Expression of TM was seen at around 100 kDa, which is in coherence with literature. The protein expression was greater in treated samples compared to the control ones.

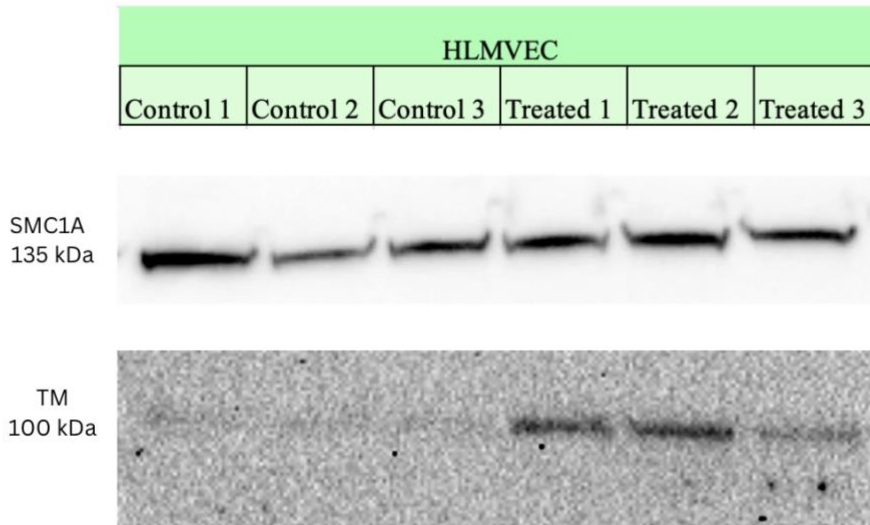

Figure 13: Increased TM expression after catecholamine stimulation in HLMVEC primary cells at 4-hour timepoint. SMC1A protein expression was equal suggesting even loading of samples. TM protein expression was detectable in all samples but significantly more in treated samples compered the control ones.

Figure 14 shows a bar graph of normalized protein expression of TM at 4-hour timepoint. The graph showed a detection of TM expression in control samples, with an increase in expression in treated samples.

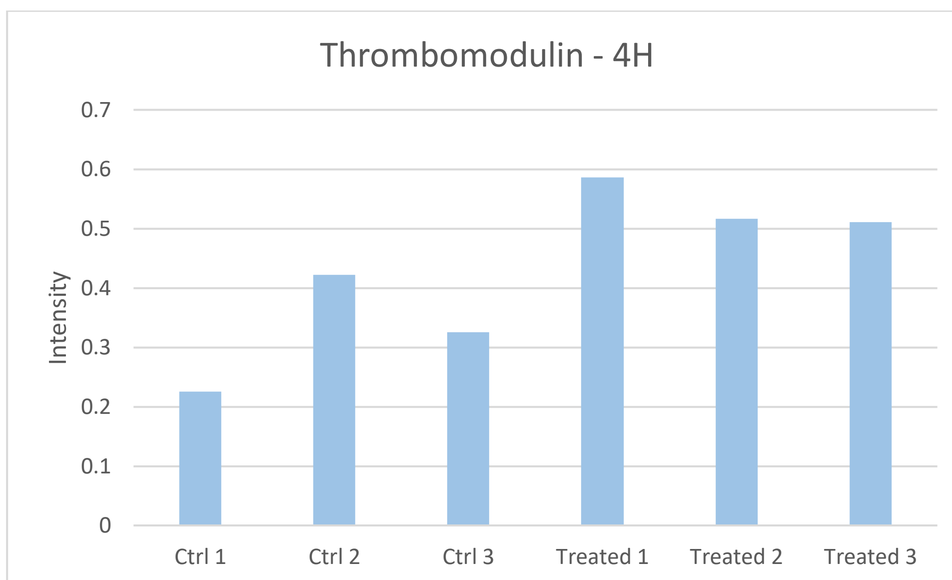

Figure 14: Normalized bar graph of increased TM expression at 4-hour timepoint in catecholamine stimulated HLMVEC cells. Visible increase in TM protein expression in samples after catecholamine stimulation compared to control samples.

The 24-hour timepoint showed similar results as the 4-hour one. *Figure 15* shows a blot for TM at 24-hour timepoint. The SMC1A blot was not successful due to unspecific bands. The protein expression of SMC1A should be around 135 kDA, as the red arrow shows.

The sample loading was not equal, despite that there was visible increase in TM expression after catecholamine stimulation.

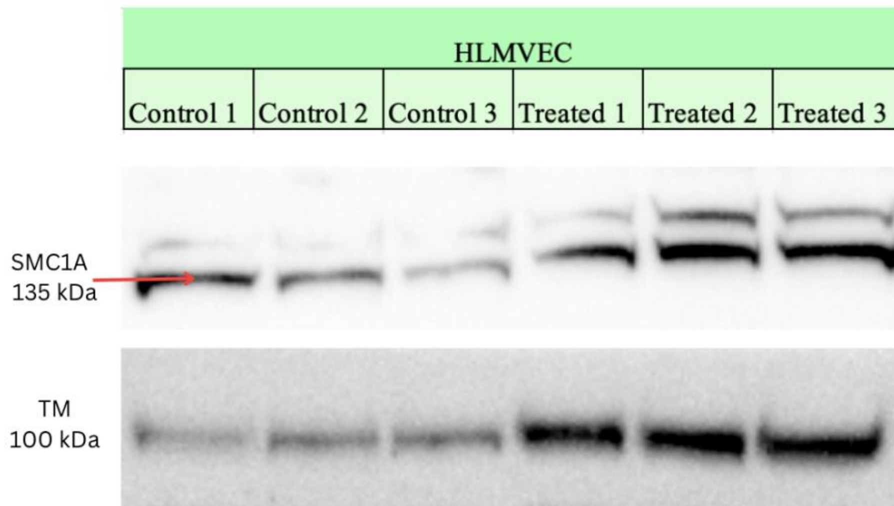

Figure 15: Increased TM expression after catecholamine stimulation in HLMVEC primary cells at 24-hour timepoint. SMC1A expression was not visibly good therefore it was hard to establish if loading was equal between samples. TM expression shows an increase after catecholamine stimulation.

Figure 16 shows a non-normalized bar graph of TM protein expression. The plot shows schematically how TM expression increases after catecholamine stimulation compared to control samples. The reason for showing a non-normalized plot is due to the inadequate protein expression of SMC1A.

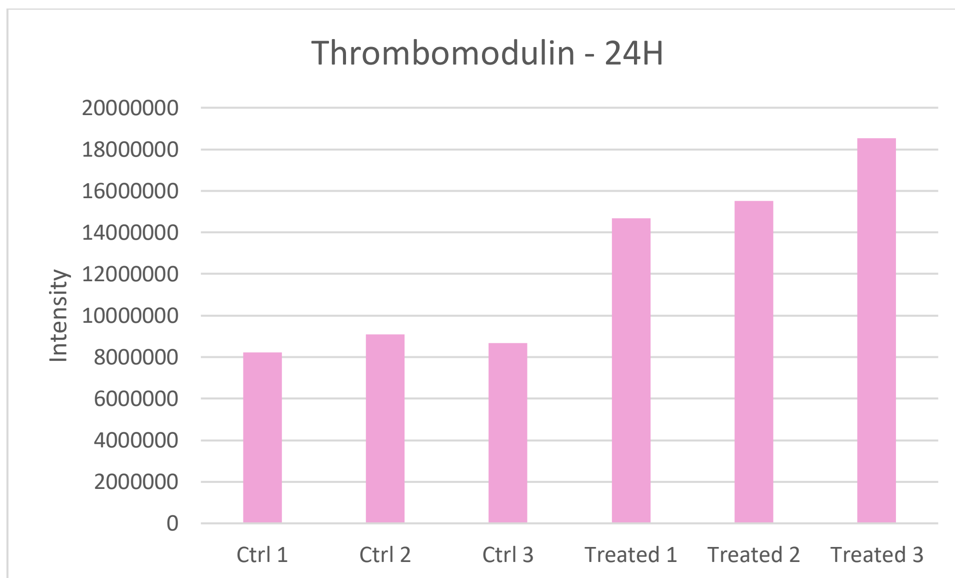

Figure 16: Non-normalized bar graph of increased TM expression at 24-hour timepoint in catecholamine stimulated HLMVEC cells. The graph shows a visible increase in TM expression compared to control.

Figure 17 shows normalized bar graph of TM protein expression at 24-hour timepoint. TM expression was normalized to expression of SMC1A. The graph shows the highest increase in control sample 3, which is not in resemblance to *figure 15.* It also shows a decrease in TM expression after treatment, which as well does not resemble *figure 15*. Unspecific bands on in the SMC1A blot could influence this change.

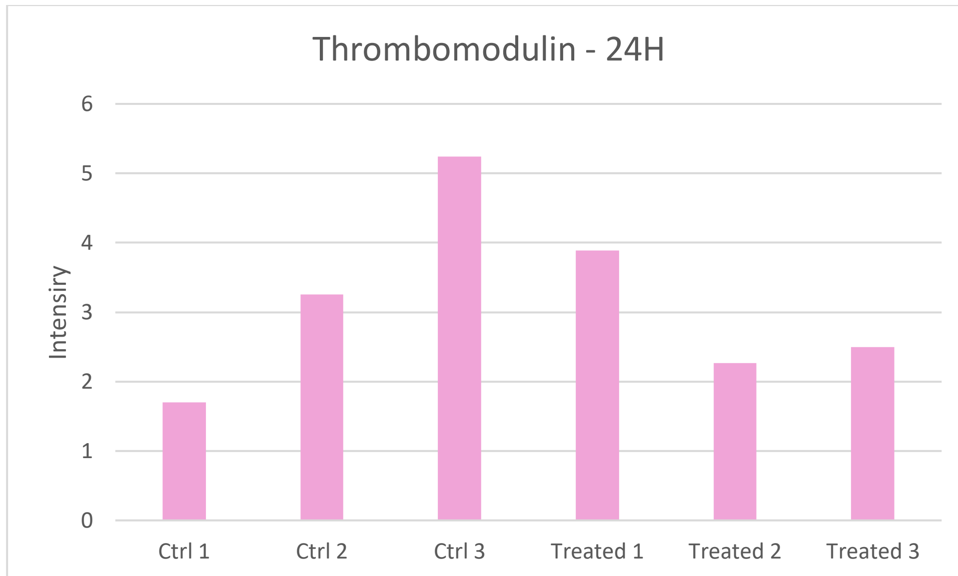

Figure 17: Normalized bar graph of increased TM expression at 24-hour timepoint in catecholamine stimulated HLMVEC cells. The graph shows a large increase in control sample 3, less in the first two. It also shows a decrease in expression after catecholamine stimulation.

3.1.3 No change in ICAM-1 expression following adrenal stimulation

Protein expression of ICAM-1 in EA.hy926 wild-type and knockout cell lines was analyzed at both timepoints after catecholamine treatment. SMC1A expression was detected at 135 kDa, which was used as a reference protein, and ICAM-1 at around 90 kDa, both in coherence to the literature. *Figure 18* shows equal SMC1A protein expression except in treated sample 3 in the wild-type cell line marked 'Treated 3'. ICAM-1 expression is equal in both wild-type and knockout samples, before and after catecholamine stimulation. Which indicates no change in expression after stimulation.

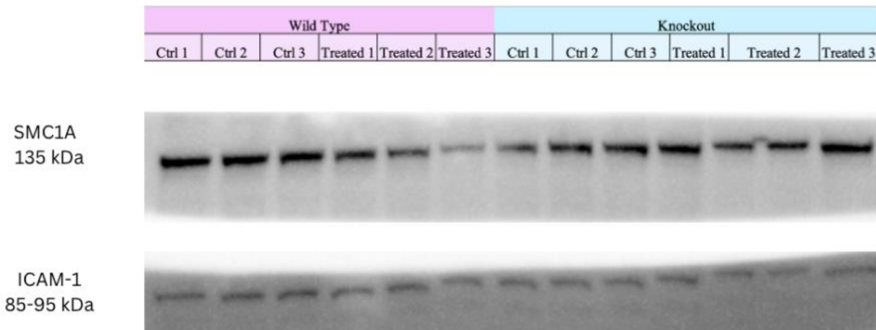

Figure 18: No change in ICAM-1 expression in EA.hy926 wild-type and knockout cell lines after catecholamine stimulation at 4-hour timepoint. SMC1A expression is equal among samples, except in treated sample 3 in wild-type line. Treated sample 2 in knockout cell line is in two wells due to a break in the well on the gel. ICAM-1 had an equal expression among all samples.

Figure 19 shows ICAM-1 protein expression at 24-hour timepoint. SMC1A was used as a reference protein. Equal loading was established due to even intensities in SMC1A bands. ICAM-1 expression was fairly equal among both cell lines, both in control and stimulated samples.

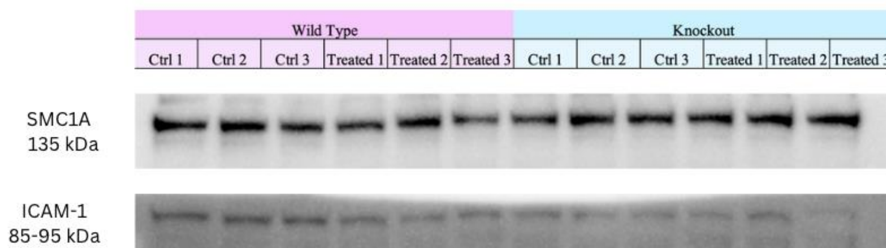

Figure 19: No change in ICAM-1 expression in EA.hy926 wild-type and knockout cell lines after catecholamine stimulation at 24-hour timepoint. SMC1A has equal intensities among all bands, which indicates equal loading of all samples. ICAM-1 protein expression was somewhat equal among all samples.

Figure 20 shows a replication of SMC1A and ICAM-1 blot at 4-hour timepoint. No significant results were established due to unspecific bands and unequal intensities in all samples. ICAM-1 protein expression is visible but unequal among samples.

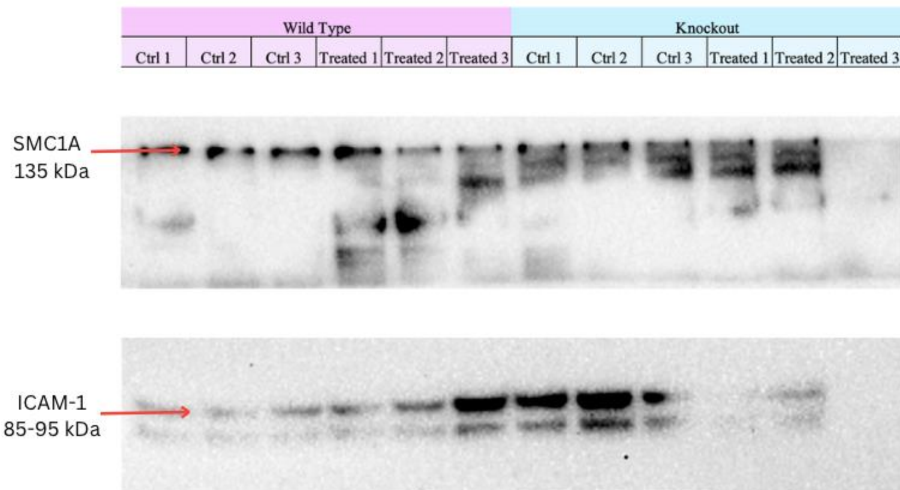

Figure 20: No change in ICAM-1 expression in EA.hy926 wild-type and knockout cell lines after catecholamine stimulation at 4-hour timepoint. No significant results could be interpreted in this blot due to unspecific bands.

Figure 21 shows a replication of SMC1A and ICAM-1 blot at 24-hour timepoint. Like in *figure 20*, no significant results could be interpreted due to unspecific bands. There was no ICAM-1 protein expression visible.

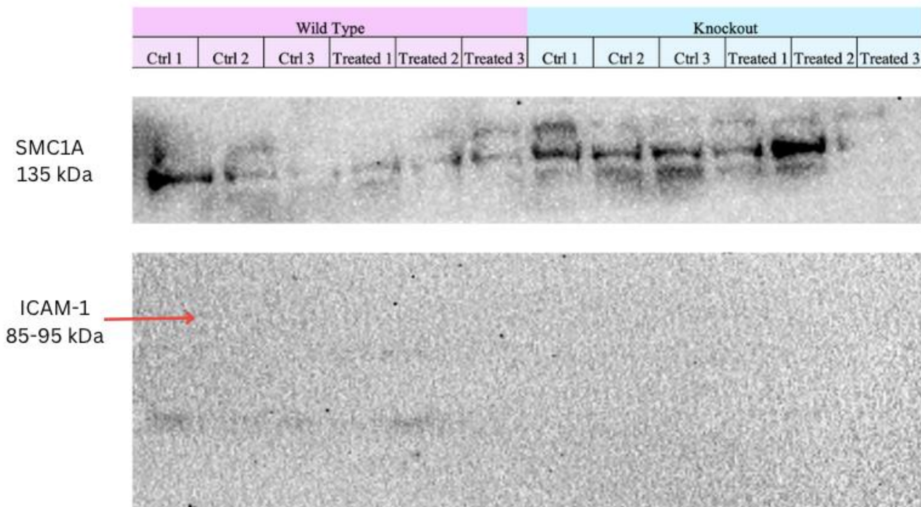

Figure 21: No change in ICAM-1 expression in EA.hy926 wild-type and knockout cell lines after catecholamine stimulation at 24-hour timepoint. No significant results could be interpreted in this blot due to unreliable intensities in the SMC1A expression. There was no ICAM-1 expression visible in this blot.

Figure 22 shows a normalized bar graph of ICAM-1 protein expression for both timepoints. The graph states that there was both an increase and decrease after catecholamine stimulation. That could have been caused by non-reliable blots.

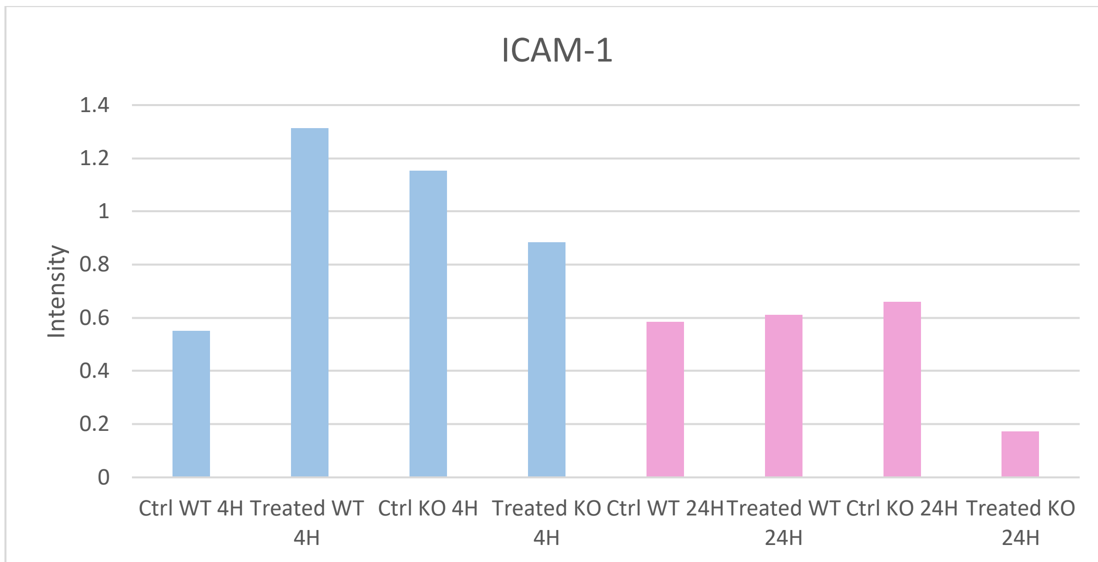

Figure 22: Normalized bar graph of ICAM-1 protein expression at both timepoints. The graph shows both an increase and decrease in protein expression after catecholamine stimulation.

3.1.4 ICAM-2 expression was inconclusive

Protein expression of ICAM-2 in EA.hy926 wild-type and knockout cell lines was blotted for at both timepoints. SMC1A expression at 135 kDa, which was used as a reference protein. According to the literature, ICAM-2 expression should be visible at around 55-80 kDa. *Figure 23* shows a blot for SMC1A and ICAM-2 at 4-hour timepoint. No visible expression of ICAM-2 was established in the blot, therefore no analytical results could be interpreted.

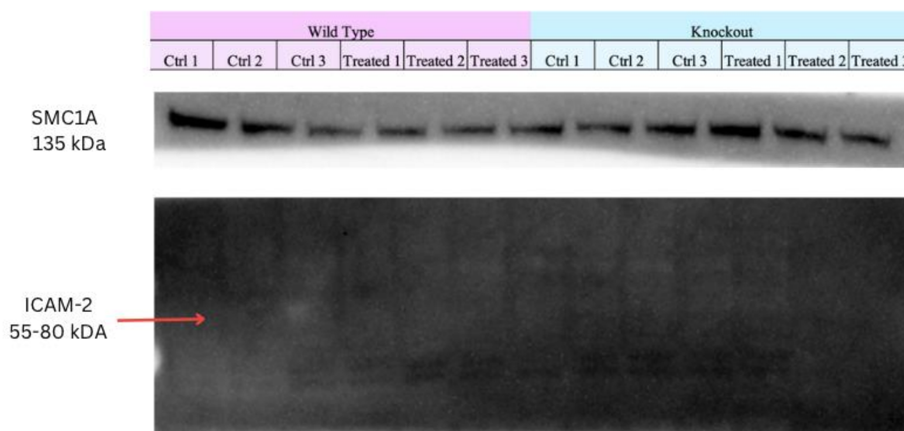

Figure 23: ICAM-2 expression in EA.hy926 wild-type and knockout cell lines was inconclusive at 4-hour timepoint. No significant results could be interpreted in this blot due to no visible expression. 1:500 ICAM-2 antibody dilution was used.

Figure 24 shows blots for SMC1A and ICAM-2 at the 24-hour timepoint. SMC1A protein expression was visible at around 135 kDa, which is consistent with the literature. No

visible expression was established for ICAM-2. No analytical results could be interpreted from the ICAM-2 blot.

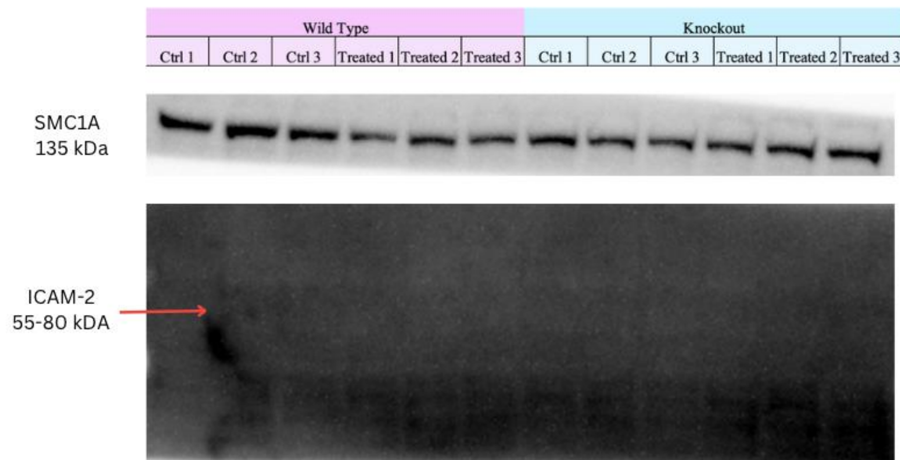

Figure 24: ICAM-2 expression in EA.hy926 wild-type and knockout cell lines was inconclusive at 24-hour timepoint. SMC1A protein expression has equal intensities, which indicate even loading of samples. No visible ICAM-2 expression was detected. 1:500 ICAM-2 antibody dilution was used.

Figure 25 shows a replication of SMC1A and ICAM-2 blot at 4-hour timepoint with different antibody dilution in comparison with *figure 23*. SMC1A protein expression was visible at around 135 kDa, which is in consistent with the literature. No visible expression was established for ICAM-2. No analytical results could be interpreted from the ICAM-2 blot.

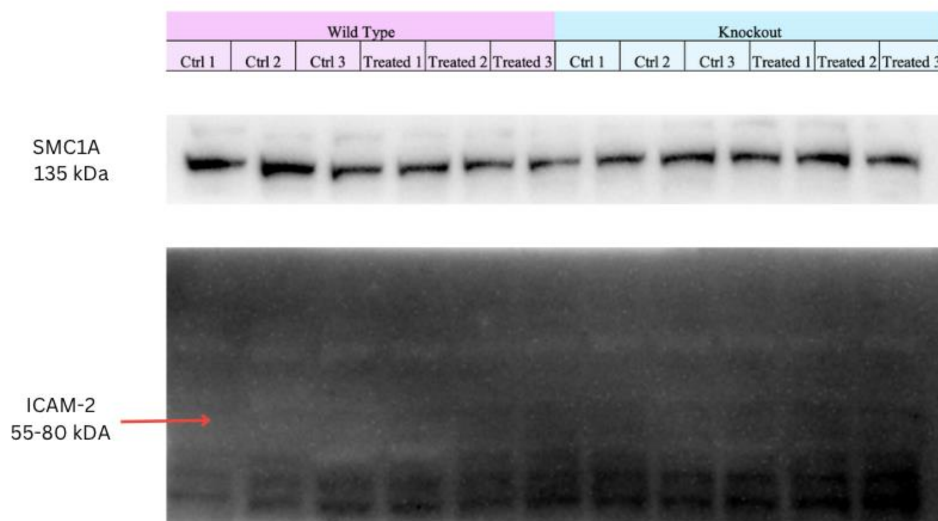

Figure 25: ICAM-2 expression in EA.hy926 wild-type and knockout cell lines was inconclusive at 4-hour timepoint. SMC1A protein expression has equal intensities which indicate even loading of sample. ICAM-2 protein expression is not visible. 1:1000 ICAM-2 antibody dilution was used.

Figure 26 shows a replication of SMC1A and ICAM-2 blot at 24-hour timepoint with different antibody dilution in comparison with *figure 24*. SMC1A protein expression is fairly equal among all samples, except in treated samples 1 and 2 in the wild-type cell line. No visible signal was detected in the ICAM-2 blot.

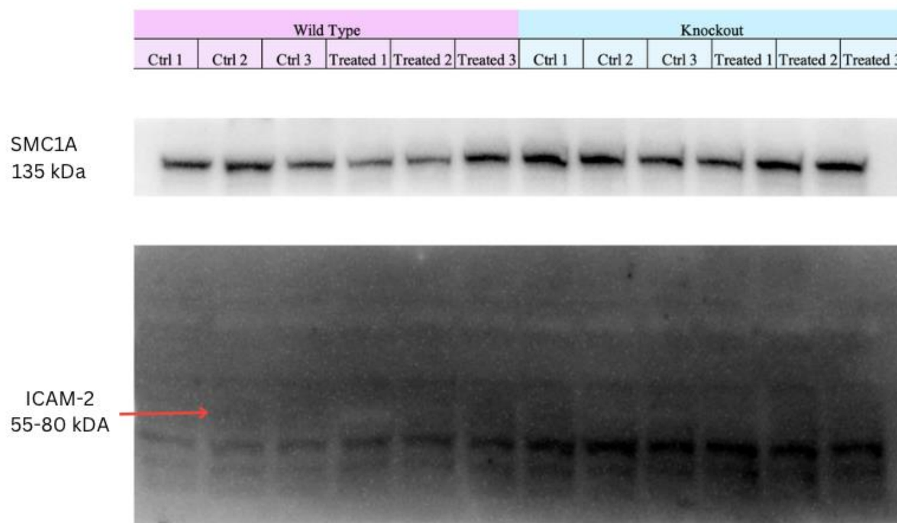

Figure 26: ICAM-2 expression in EA.hy926 wild-type and knockout cell lines was inconclusive at 24-hour timepoint. SMC1A protein expression has equal intensities which indicate even loading of sample. ICAM-2 protein expression is not visible. 1:1000 ICAM-2 antibody dilution was used.

3.1.5 VCAM-1 expression was inconclusive

Protein expression of VCAM-1 in EA.hy926 wild-type and knockout cell lines was analyzed at both timepoints after catecholamine treatment. Beta-tubulin expression was established at 55 kDa, which was used as a reference protein. Theoretically VCAM-1 protein expression should be at around 100 kDa. *Figure 27* shows protein expression at 4-hour timepoint. Beta-tubulin expression was inconclusive due to signals only being visible in the wild-type samples and not in the knockout samples. VCAM-1 protein expression was non-visible in the blot. No analytical results could be interpreted.

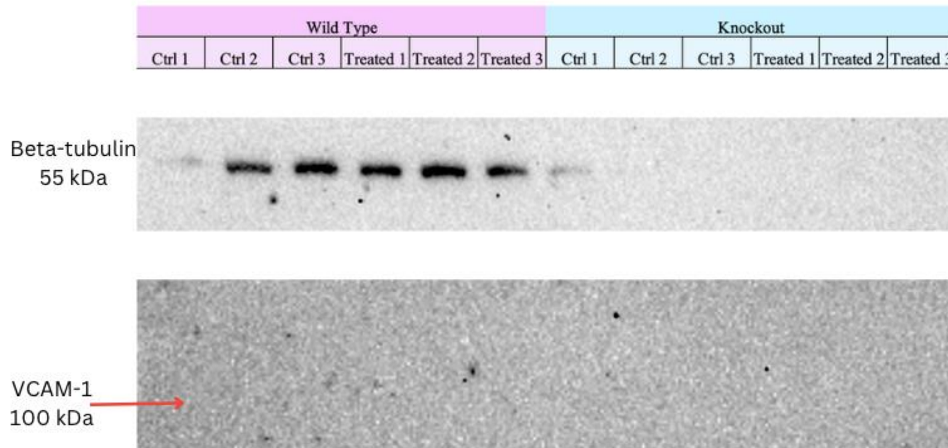

Figure 27: VCAM-2 expression in EA.hy926 wild-type and knockout cell lines was inconclusive at 4-hour timepoint. Beta-tubulin protein expression is visible in wild-type samples, with a faint band in control sample 1. It is non-existent in all knockout samples except a faint band in knockout control sample 1. Protein expression of VCAM-1 was not visible in the blot.

Figure 28 shows protein expression at 24-hour timepoint. No protein expression was visible in beta-tubulin or VCAM-1, thereby no results could be interpreted. Theoretically bands would have shown at around 55 kDa for beta-tubulin and 100 kDa for VCAM-1.

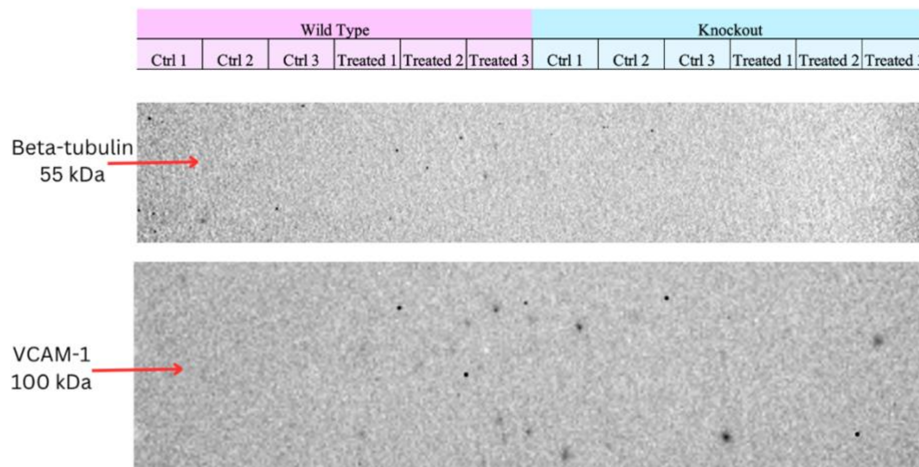

Figure 28: VCAM-2 expression in EA.hy926 wild-type and knockout cell lines was inconclusive at 24-hour timepoint. No protein expression was detected in both samples. Bands should have shown at 55 kDa for beta-tubulin and 100 kDa for VCAM-1.

3.1.6 CREBp expression was inconclusive

Protein expression of phosphorylated CREB (CREBp) in EA.hy926 wild-type and knockout cell lines was blotted for at both timepoints after catecholamine treatment. SMC1A expression is theoretically at 135 kDa and CREBp at 40 kDa. *Figure 29* shows an

equal amount of loading of samples, except in treated sample 3 in the wild-type cell line. SMC1A protein expression was detected at 135 kDa. Treated sample 2 in knockout cell had visible bands in two wells, due to rupture in gel. No protein expression was detected for CREBp. Thereby no analytical results could be interpreted.

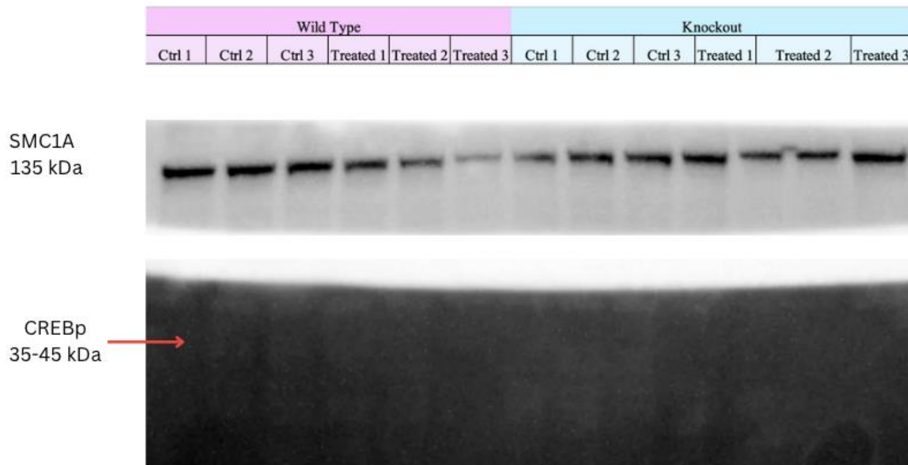

Figure 29: CREBp protein expression in EA.hy926 wild-type and knockout cell lines was inconclusive at 4-hour timepoint. SMC1A protein expression fairly equal among samples, except treated sample 3 in wild-type cell line. No visible protein expression was detected in CREBp. 1:4000 CREBp antibody dilution was used.

Figure 30 shows SMC1A expression at 135 kDa, which was used as a reference protein, and CREBp at around 40 kDa. SMC1A protein expression shows an equal amount of loading as seen in intensities of bands. No protein expression was detected for CREBp. Thereby no analytical results could be interpreted from that blot.

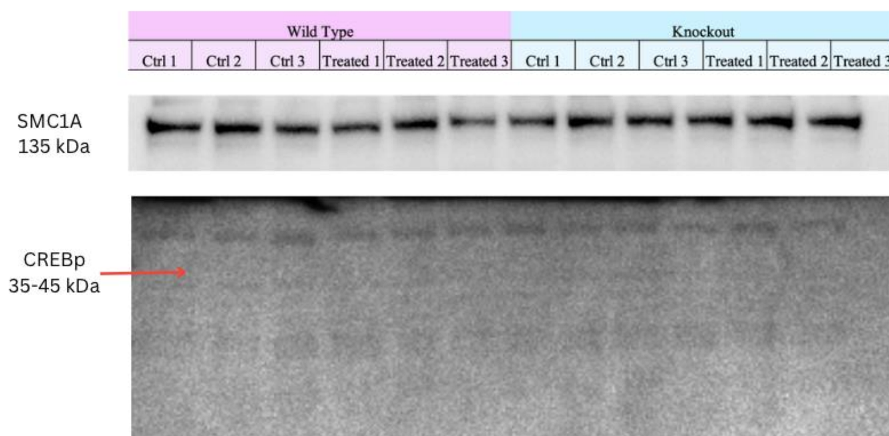

Figure 30: CREBp protein expression in EA.hy926 wild-type and knockout cell lines was inconclusive at 24-hour timepoint. SMC1A protein expression equal among samples. No visible protein expression was detected in CREBp. 1:4000 CREBp antibody dilution was used.

Figure 31 shows SMC1A expression at 135 kDa, which was used as a reference protein, and CREBp at around 40 kDa. SMC1A protein expression shows an equal amount of loading as seen in intensities of bands. No visible protein expression was detected for CREBp. Thereby no analytical results could be interpreted from that blot.

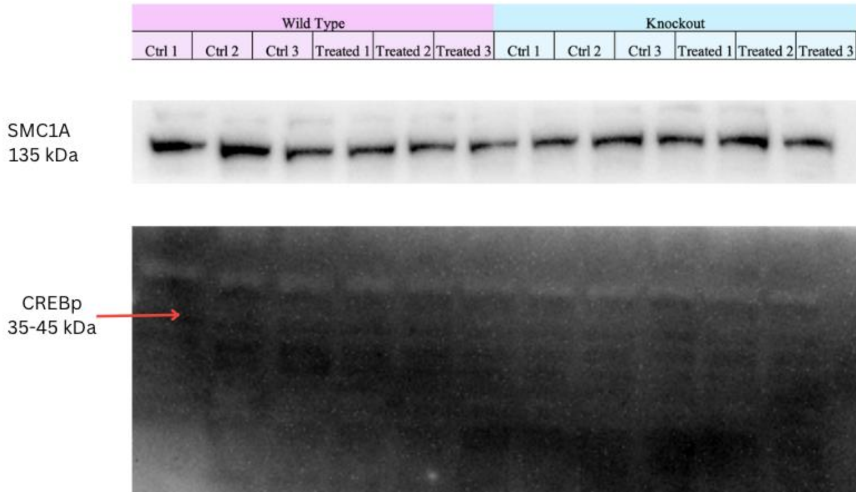

Figure 31: CREBp protein expression in EA.hy926 wild-type and knockout cell lines was inconclusive at 4-hour timepoint. SMC1A protein expression equal among samples, No visible protein expression was detected in CREBp. 1:8000 CREBp antibody dilution was used.

Figure 32 shows SMC1A expression at 135 kDa, which was used as a reference protein, and CREBp at around 40 kDa. SMC1A protein expression shows a fairly equal amount of loading, except in treated samples 1 and 2 in wild-type cell line. No protein expression was detected for CREBp. Thereby no analytical results could be interpreted from that blot.

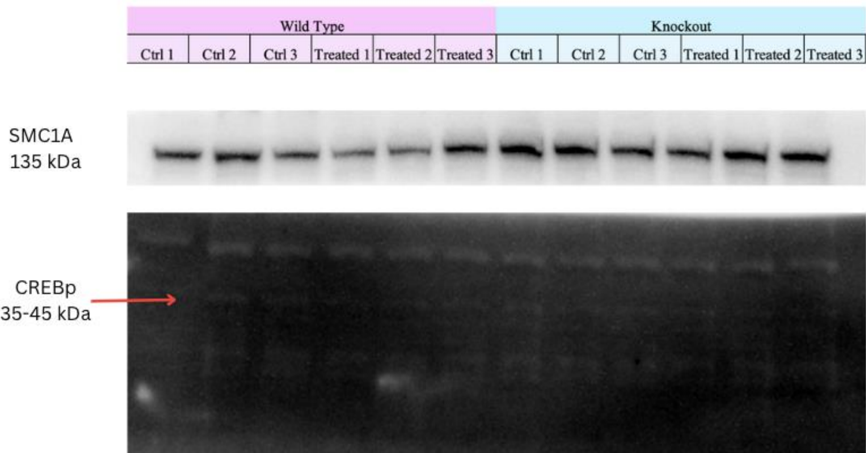

Figure 32: CREBp protein expression in EA.hy926 wild-type and knockout cell lines was inconclusive at 24-hour timepoint. SMC1A protein expression fairly equal among samples. No visible protein expression was detected in CREBp. 1:8000 CREBp antibody dilution was used.

3.1.7 VEGF-A expression was inconclusive

Protein expression of VEGF-A in EA.hy926 wild-type and knockout cell lines was blotted for at both timepoints after catecholamine treatment. *Figure 33* shows a SMC1A protein expression at 135 kDa, which was used as a reference protein. SMC1A expression was fairly equal which suggested even loading of samples. No visible VEGF-A protein expression was detected, theoretically the band should have shown at around 27 kDa. Unspecific bands were visible at around 35 kDa both in *figure 33* and *34*.

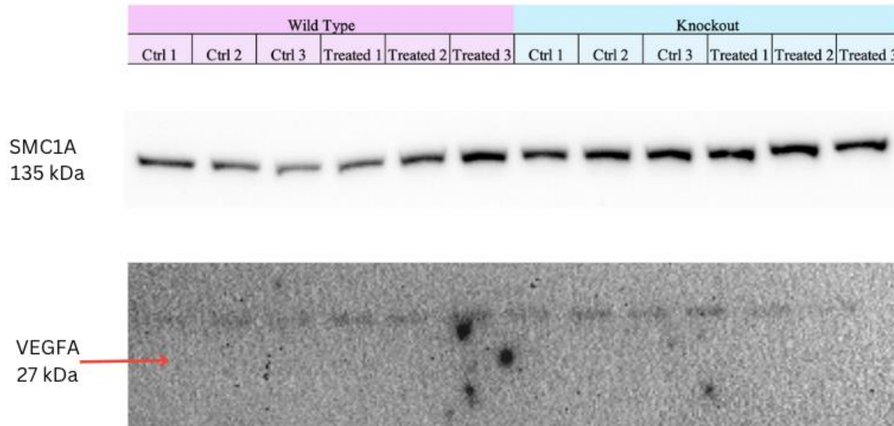

Figure 33:VEGF-A protein expression in EA.hy926 wild-type and knockout cell lines was inconclusive at 4-hour timepoint. Showing SMC1A protein expression at 135 kDa. No VEGF-A expression was detected.

Figure 34 shows SMC1A expression at 135 kDa, which was used as a reference protein. Equal loading was established due to even intensities across all samples. VEGF-A expression was not detected, like in *figure 33,* theoretical expression should be detected around 27 kDa. Therefore, no results could be analyzed from this blot.

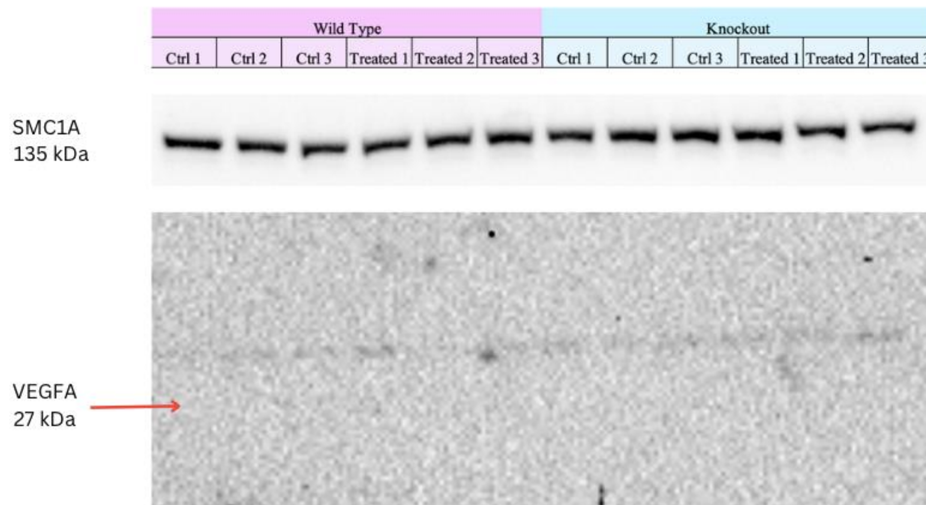

Figure 34: VEGF-A protein expression in EA.hy926 wild-type and knockout cell lines was inconclusive at 24-hour timepoint. Showing SMC1A protein expression at 135 kDa. No VEGF-A expression was detected.

In conclusion, the results provided insight in expression of endothelial dysfunction target proteins. The main finding in the results was the increase in protein expression of CA2 and thrombomodulin in HLMVEC cells after catecholamine stimulation. Protein expression in EA.hy926 cell lines did not yield results that could be interpreted. Those problems could be due to antibody sensitivity, experimental conditions, or insufficient blocking incubation.

4 Discussions

The primary research question addressed in the project was whether GRAMD1B upregulates or downregulates the expression of CA2, CREBp, ICAM-1, ICAM-2, TM, VCAM-1 and VEGF-A proteins following catecholamine stimulation. The goal was to see an increase in protein expression on Western blots. HLMVEC primary cells and EA.hy926 wild-type and knockout lines were used to establish the protein expression of aforementioned proteins. CA2 and TM showed an increase in protein expression after catecholamine stimulation in HLMVEC cells. Which was expected from the interpretation of RNA-sequencing data from earlier research that showed an increase in gene-expression after catecholamine stimulation. Protein expression of CA2 and TM was not established in EA.hy926 cell lines, therefore GRAMD1B influence could not be established in those blots.

Western blots using the EA.hy926 cell lines did not yield expected results. ICAM-1 protein expression was visible but showed faint bands on the Western blots. No upregulation was detected therefore the Western blot must be repeated for better results that can be interpreted and analysed. ICAM-2 did not show any visible bands on the Western blot. Blot was repeated two times, with different antibody dilutions. Further optimizing must be established regarding ICAM-2. The VCAM-1 Western blots did not yield any results as there were no visible bands. Beta-tubulin reference protein also showed no significant bands. Like ICAM-2, the Western blot must be optimized to yield better results. Phosphorylated CREB yielded black membranes, which is likely due to overexposure of primary antibodies or not long enough blocking incubation time. The Western blot was repeated with different antibody dilutions, both yielding black membranes. Black membranes could also be due to membranes drying up. The VEGF-A Western blot had unspecific protein binding and no visible VEGF-A bands. Which could be due to antibody defect or insignificant blocking period.

Overall, the Western blot of CA2 and TM with HLMVEC cells were successful and could be interpreted analytically. One limitation in the research project were inconsistency of protein band visibility in the Western blot conducted with the EA.hy926 cell lines, which require further optimization for blotting conditions. Future directions in this study requires further antibody detection and additional replicates of Western blots to gain more knowledge about understanding how the proteins relate to vascular diseases. If time was

not a factor, I would conduct further Western blots with CA2 and TM in EA.hy926 cell lines and see if GRAMD1B implements any changes in the protein expression. Overall, this research has highlighted the importance of further optimizing our understanding of how GRAMD1B influences endothelial cell response to catecholamines. This project provides a good foundation for future research aimed at developing therapeutic solutions for endothelial dysfunction and SHINE.

References

Aird, W. C. (2004). Endothelium as an organ system: *Critical Care Medicine*, *32*(Supplement), S271–S279. https://doi.org/10.1097/01.CCM.0000129669.21649.40

Alberts, B., Heald, R., Johnson, A., Morgan, D., Raff, M., Roberts, K., & Walter, P. (2022). *Molecular Biology of the Cell: Seventh International Student Edition with Registration Card*. W. W. Norton. https://books.google.is/books?id=xLqazgEACAAJ

Alberts, B., Johnson, A., Lewis, J., Raff, M., Roberts, K., & Walter, P. (2002). Blood Vessels and Endothelial Cells. In *Molecular Biology of the Cell. 4th edition*. Garland Science. https://www.ncbi.nlm.nih.gov/books/NBK26848/

Alver, A., Şentürk, A., Çakirbay, H., Menteşe, A., Gökmen, F., Keha, E. E., & Uçar, F. (2011). Carbonic anhydrase II autoantibody and oxidative stress in rheumatoid arthritis. *Clinical Biochemistry*, *44*(17–18), 1385–1389. https://doi.org/10.1016/j.clinbiochem.2011.09.014

Amsellem, V., Dryden, N. H., Martinelli, R., Gavins, F., Almagro, L. O., Birdsey, G. M., Haskard, D. O., Mason, J. C., Turowski, P., & Randi, A. M. (2014). ICAM-2 regulates vascular permeability and N-cadherin localization through ezrin-radixin-moesin (ERM) proteins and Rac-1 signalling. *Cell Communication and Signaling*, *12*(1), 12. https://doi.org/10.1186/1478-811X-12-12

Andreis, D. T., & Singer, M. (2016). Catecholamines for inflammatory shock: A Jekyll-and-Hyde conundrum. *Intensive Care Medicine*, *42*(9), 1387–1397. https://doi.org/10.1007/s00134-016-4249-z

Boffa, M.-C., & Karmochkine, M. (1998). Thrombomodulin: An overview and potential implications in vascular disorders. *Lupus*, *7*(2_suppl), 120–125. https://doi.org/10.1177/096120339800700227

Britten, M. W., Lümers, L., Tominaga, K., Peters, J., & Dirkmann, D. (2021). Glycocalyx components affect platelet function, whole blood coagulation, and fibrinolysis: An in vitro

study suggesting a link to trauma-induced coagulopathy. *BMC Anesthesiology*, *21*(1), 83. https://doi.org/10.1186/s12871-021-01300-1

Bui, T. M., Wiesolek, H. L., & Sumagin, R. (2020). ICAM-1: A master regulator of cellular responses in inflammation, injury resolution, and tumorigenesis. *Journal of Leukocyte Biology*, *108*(3), 787–799. https://doi.org/10.1002/JLB.2MR0220-549R

Campbell, H. K., Maiers, J. L., & DeMali, K. A. (2017). Interplay between tight junctions & adherens junctions. *Experimental Cell Research*, *358*(1), 39–44. https://doi.org/10.1016/j.yexcr.2017.03.061

Chignalia, A. Z., Yetimakman, F., Christiaans, S. C., Unal, S., Bayrakci, B., Wagener, B. M., Russell, R. T., Kerby, J. D., Pittet, J.-F., & Dull, R. O. (2016). THE GLYCOCALYX AND TRAUMA: A REVIEW. *Shock*, *45*(4), 338–348. https://doi.org/10.1097/SHK.0000000000000513

De Bock, K., Georgiadou, M., Schoors, S., Kuchnio, A., Wong, B. W., Cantelmo, A. R., Quaegebeur, A., Ghesquière, B., Cauwenberghs, S., Eelen, G., Phng, L.-K., Betz, I., Tembuyser, B., Brepoels, K., Welti, J., Geudens, I., Segura, I., Cruys, B., Bifari, F., … Carmeliet, P. (2013). Role of PFKFB3-Driven Glycolysis in Vessel Sprouting. *Cell*, *154*(3), 651–663. https://doi.org/10.1016/j.cell.2013.06.037

Dyer, L. A., & Patterson, C. (2010). Development of the Endothelium: An Emphasis on Heterogeneity. *Seminars in Thrombosis and Hemostasis*, *36*(3), 227–235. https://doi.org/10.1055/s-0030-1253446

EA.hy926—CRL-2922 | ATCC. (n.d.). Retrieved April 18, 2024, from https://www.atcc.org/products/crl-2922

Eichmann, A., & Simons, M. (2012). VEGF signaling inside vascular endothelial cells and beyond. *Current Opinion in Cell Biology*, *24*(2), 188–193. https://doi.org/10.1016/j.ceb.2012.02.002

Endemann, D. H., & Schiffrin, E. L. (2004). Endothelial Dysfunction. *Journal of the American Society of Nephrology*, *15*(8), 1983. https://doi.org/10.1097/01.ASN.0000132474.50966.DA

Figueroa, X. F., & Duling, B. R. (2009). Gap Junctions in the Control of Vascular Function. *Antioxidants & Redox Signaling*, *11*(2), 251–266. https://doi.org/10.1089/ars.2008.2117

Gonzalez Rodriguez, E., Ostrowski, S. R., Cardenas, J. C., Baer, L. A., Tomasek, J. S., Henriksen, H. H., Stensballe, J., Cotton, B. A., Holcomb, J. B., Johansson, P. I., & Wade, C. E. (2017).

Syndecan-1: A Quantitative Marker for the Endotheliopathy of Trauma. *Journal of the American College of Surgeons*, *225*(3), 419–427. https://doi.org/10.1016/j.jamcollsurg.2017.05.012

Human Lung Microvascular Endothelial Cells, HMVEC-L | Lonza. (n.d.). Retrieved April 18, 2024, from https://bioscience.lonza.com/lonza_bs/IS/en/Primary-and-Stem-Cells/p/000000000000184961/HMVEC-L-%E2%80%93-Human-Lung-Microvascular-Endothelial-Cells

ICAM2—Intercellular adhesion molecule 2—Homo sapiens (Human) | UniProtKB | UniProt. (n.d.). Retrieved April 9, 2024, from https://www.uniprot.org/uniprotkb/P13598/entry

Johansson, P. I., Stensballe, J., Rasmussen, L. S., & Ostrowski, S. R. (2011). A High Admission Syndecan-1 Level, A Marker of Endothelial Glycocalyx Degradation, Is Associated With Inflammation, Protein C Depletion, Fibrinolysis, and Increased Mortality in Trauma Patients. *Annals of Surgery*, *254*(2), 194. https://doi.org/10.1097/SLA.0b013e318226113d

Johansson, P., Stensballe, J., & Ostrowski, S. (2017). Shock induced endotheliopathy (SHINE) in acute critical illness—A unifying pathophysiologic mechanism. *Critical Care*, *21*(1), 25. https://doi.org/10.1186/s13054-017-1605-5

Kong, D.-H., Kim, Y. K., Kim, M. R., Jang, J. H., & Lee, S. (2018). Emerging Roles of Vascular Cell Adhesion Molecule-1 (VCAM-1) in Immunological Disorders and Cancer. *International Journal of Molecular Sciences*, *19*(4), 1057. https://doi.org/10.3390/ijms19041057

Konukoglu, D., & Uzun, H. (2017). Endothelial Dysfunction and Hypertension. *Advances in Experimental Medicine and Biology*, *956*, 511–540. https://doi.org/10.1007/5584_2016_90

López García de Lomana, A., Vilhjálmsson, A. I., McGarrity, S., Sigurðardóttir, R., Anuforo, Ó., Viktorsdóttir, A. R., Kotronoulas, A., Bergmann, A., Franzson, L., Halldórsson, H., Henriksen, H. H., Wade, C. E., Johansson, P. I., & Rolfsson, Ó. (2022). Metabolic Response in Endothelial Cells to Catecholamine Stimulation Associated with Increased Vascular Permeability. *International Journal of Molecular Sciences*, *23*(6), 3162. https://doi.org/10.3390/ijms23063162

Martz, E. (1998). Lymphocyte Function-Associated Antigen 1 (LFA-1). In *Encyclopedia of Immunology* (pp. 1607–1612). Elsevier. https://doi.org/10.1006/rwei.1999.0411

McFarlane, M. R., Liang, G., & Engelking, L. J. (2014). Insig Proteins Mediate Feedback Inhibition of Cholesterol Synthesis in the Intestine. *The Journal of Biological Chemistry*, *289*(4), 2148–2156. https://doi.org/10.1074/jbc.M113.524041

Michiels, C. (2003). Endothelial cell functions. *Journal of Cellular Physiology*, *196*(3), 430–443. https://doi.org/10.1002/jcp.10333

Mozafari, H., Zhou, C., & Gu, L. (2019). Mechanical contribution of vascular smooth muscle cells in the tunica media of artery. *Nanotechnology Reviews*, *8*(1), 50–60. https://doi.org/10.1515/ntrev-2019-0005

Nagy, J. A., Dvorak, A. M., & Dvorak, H. F. (2007). VEGF-A and the Induction of Pathological Angiogenesis. *Annual Review of Pathology: Mechanisms of Disease*, *2*(1), 251–275. https://doi.org/10.1146/annurev.pathol.2.010506.134925

Naito, T., & Saheki, Y. (2021). GRAMD1-mediated accessible cholesterol sensing and transport. *Biochimica et Biophysica Acta (BBA) - Molecular and Cell Biology of Lipids*, *1866*(8), 158957. https://doi.org/10.1016/j.bbalip.2021.158957

Paravati, S., Rosani, A., & Warrington, S. J. (2024). Physiology, Catecholamines. In *StatPearls*. StatPearls Publishing. http://www.ncbi.nlm.nih.gov/books/NBK507716/

Pierce^{TM} BCA Protein Assay Kits. (n.d.). Retrieved April 18, 2024, from https://www.thermofisher.com/order/catalog/product/23225

Reitsma, S., Slaaf, D. W., Vink, H., van Zandvoort, M. A. M. J., & oude Egbrink, M. G. A. (2007). The endothelial glycocalyx: Composition, functions, and visualization. *Pflügers Archiv - European Journal of Physiology*, *454*(3), 345–359. https://doi.org/10.1007/s00424-007-0212-8

Shah, G. N., Price, T. O., Banks, W. A., Morofuji, Y., Kovac, A., Ercal, N., Sorenson, C. M., Shin, E. S., & Sheibani, N. (2013). Pharmacological Inhibition of Mitochondrial Carbonic Anhydrases Protects Mouse Cerebral Pericytes from High Glucose-Induced Oxidative Stress and Apoptosis. *Journal of Pharmacology and Experimental Therapeutics*, *344*(3), 637–645. https://doi.org/10.1124/jpet.112.201400

Weis, S. M., & Cheresh, D. A. (2005). Pathophysiological consequences of VEGF-induced vascular permeability. *Nature*, *437*(7058), 497–504. https://doi.org/10.1038/nature03987

Witter, K., Tonar, Z., & Schöpper, H. (2017). How many Layers has the Adventitia? – Structure of the Arterial Tunica Externa Revisited. *Anatomia, Histologia, Embryologia*, *46*(2), 110–120. https://doi.org/10.1111/ahe.12239

Zhang, H., Kong, Q., Wang, J., Jiang, Y., & Hua, H. (2020). Complex roles of cAMP–PKA–CREB signaling in cancer. *Experimental Hematology & Oncology*, *9*(1), 32. https://doi.org/10.1186/s40164-020-00191-1